NASA Technical Memorandum 89106

COMPUTATIONAL METHODS FOR UNSTEADY TRANSONIC FLOWS

J. W. EDWARDS
AND
J. L. THOMAS

MARCH 1987

National Aeronautics and
Space Administration

Langley Research Center
Hampton, Virginia 23665

COMPUTATIONAL METHODS FOR UNSTEADY TRANSONIC FLOWS

John W. Edwards*

and

James L. Thomas**
NASA Langley Research Center
Hampton, Virginia 23665

Abstract

Computational methods for unsteady transonic flows are surveyed with emphasis upon applications to aeroelastic analysis and flutter prediction. Computational difficulty is discussed with respect to type of unsteady flow; attached, mixed (attached/separated) and separated. Significant early computations of shock motions, aileron buzz and periodic oscillations are discussed. The maturation of computational methods towards the capability of treating complete vehicles with reasonable computational resources is noted and a survey of recent comparisons with experimental results is compiled. The importance of mixed attached and separated flow modeling for aeroelastic analysis is discussed and recent calculations of periodic aerodynamic oscillations for an 18 percent thick circular arc airfoil are given.

Introduction

In the past decade there has been much activity in the development of computational methods for the analysis of unsteady transonic aerodynamics about airfoils and wings. Advances have parallelled developments in steady computational fluid dynamics (CFD) with a lag of approximately five years[1] due to the additional requirement of time-accuracy. Figure 1, taken from the specification document for U.S. military aircraft[2], illustrates significant features which must be addressed in the treatment of computational transonic unsteady aerodynamics. On the plot of equivalent airspeed versus Mach number, lines of constant altitude are straight lines through the origin with decreasing altitudes represented by steeper slopes. The flight envelope is typically set by the maximum limit speed and a typical flutter boundary curve, characterized by the flutter speed gradually dropping to a minimum in the transonic speed range followed by a rapid upward rise, is shown. The ability to predict this minimum, termed the transonic flutter dip, is of great importance in design, since the flutter boundary must be shown by a combination of analysis and flight test to be outside the flight envelope by a margin of at least 15 percent in equivalent airspeed, i.e. the flutter boundary must be outside the dashed line boundary in fig. 1. Subsonic linear unsteady aerodynamic theories have been reasonably successful in predicting this flutter boundary for Mach numbers up to 0.6-0.7 but linear theory is unable to account for the effect of aerodynamic shape and maneuvering condition upon unsteady airloads. At higher Mach numbers linear analysis has been used with more or less success depending upon the severity of local transonic effects. The occurrence of flutter within the flight envelope of an aircraft usually leads to structural failure and loss of the vehicle, highlighting the necessity for careful validation of computational methods intended for use in this area. This is a key difference in the utilization of steady and unsteady computational methods which must be clearly understood.

This paper attempts to provide an assessment of the current situation regarding computational methods for transonic unsteady aerodynamics. It is written from the perspective of aeroelastic applications and the prediction of aircraft flutter. Thus attention is devoted to assessing the state-of-the-art for predicting unsteady airloads upon oscillating lifting surfaces. Also, there is much current interest in airflows over rigid surfaces which exhibit periodic unsteadiness over narrow Mach number regions. The interaction of these two types of flows are likely to be of great interest in the near future as computational aeroelasticity matures. We have restricted this survey to computational methods which solve time-accurate transonic flow equations. Harmonic perturbation and other approximate solution methods have been an active research area and an assessment of their relative merits vis a vis time-accurate solutions would be valuable. Also not covered are unsteady three-dimensional vortex flows since this field is currently undergoing a rapid growth[3].

This field received an initial impetus in the mid-1970's from three sources: Tijdeman's[4] pioneering experimental work on transonic unsteady pressure measurements, Magnus and Yoshihara's demonstration of key transonic flow features for an airfoil with an oscillating flap[5] and the introduction of an economical transonic finite-difference solution algorithm by Ballhaus and Goorjian[6]. Ballhaus[7] gives a survey of the field from this period. The AGARD Structures and Materials Panel Subcommittee on Aeroelasticity has selected experimental unsteady pressure data sets and defined two- and three-dimensional Standard Aeroelastic Configurations[8,9] to provide reference computational test cases for the development and validation of improved computational methods. The data sets were obtained from rigid models undergoing pitch and control surface

*Head, Unsteady Aerodynamics Branch, Loads and Aeroelasticity Division, Member AIAA.
**Senior Research Scientist, Analytical Methods Branch, Transonic Aerodynamics Division, Member AIAA.

oscillations and includes both conventional and supercritical airfoil geometries[10,11,12]. In addition to these data sets, Sandford et al.[13] summarize a series of unsteady pressure tests made at NASA Langley and Tijdeman[14] presents a much used data set for a fighter wing configuration.

Computational methods have been pursued at a number of differing levels of physical approximation to the flow equations. Magnus and Yoshihara[5,15,16] used an explicit algorithm to solve the Euler (EE) equations. Steger and Bailey[17] reported a significant early application to the problem of aileron buzz using an implicit approximate factorization solution algorithm for the Navier-Stokes (NS) equations. Chyu and his coauthors[18,19] have pursued further applications of derivatives of this code. Most of the nonlinear unsteady computations to date have been made by solving the potential equations, both with and without interacted viscous effects. For example, the alternating-direction implicit (ADI) algorithm embodied in the LTRAN2 code of Balihaus and Goorjian[6] enabled efficient solutions of the two-dimensional low frequency transonic small disturbance (TSD) potential equation through the use of large time steps. Extensions of this ADI algorithm have been widely used by many researchers. A semi-implicit form of the ADI algorithm is used in the 3-D XTRAN3S code[20,21] developed for the aeroelastic analysis of wings. Other TSD and Full Potential (FP) equation codes are described in Refs. 22-27. There is a growing trend, especially for steady flows, towards use of the Euler equations rather than the potential equations. Euler equation codes treating 2-D oscillating airfoils are reported in Refs. 28-32 while Salmond[33] and Belk[34] show results from 3-D Euler codes.

Over this same time period, several experimental investigations of periodic aerodynamic flows about rigid airfoils have been reported. McDevitt[35,36] documented such conditions for a very narrow range of Mach number for an 18 percent thick circular arc airfoil and Levy[37] reproduced the effect with calculations from a NS code. Subsequently, Mabey[38] studied these oscillations for circular arc airfoils with thicknesses of 10-20 percent. References 39 and 40 give details for a 14 percent circular arc airfoil. Related information regarding the interaction of unsteady airloads caused by transitional boundary layers with structural oscillations is given by Mabey et al.[41] Another class of separation-induced periodic flow problems, vortex shedding about rigid cylinders and airfoils at high angle-of-attack, has been studied using NS codes for a variety of Reynolds numbers in Refs. 42-44.

Unsteady aerodynamics has been the theme of four recent AGARD conferences[45-48] whose proceedings contain a wealth of information. Survey papers focusing upon computational requirements and resources are given by Peterson[49] and McCroskey et al.[1]. Summary papers of the 1984 and 1985 AGARD conferences are given by Mykytow[50] and by Mabey and Chambers[51]. The latter reference makes recommendations regarding computational and experimental methods for unsteady flow phenomena and draws particular attention to the need to pay careful attention to the nature of shock motions. The periodic oscillations about circular arc airfoils are recommended as benchmark computational cases for all time-dependent transonic viscous flow theories. Zwaan[52] surveys aeroelastic problems in transonic flow while Deiwert[53] reviews the numerical simulation of unsteady interactive flows. Finally, Mabey[54] gives a review of pertinent experimental research on time-dependent aerodynamics.

In the following sections, the distinction between attached and separated flow conditions and the available experimental data sets are discussed. A brief discussion of the hierarchy of available flow solvers is given with attention to details specific to unsteady flows. Then, computational capability for two-dimensional and three-dimensional unsteady aerodynamics is illustrated, followed by a brief review of aeroelastic applications. Finally, computations of unsteady periodic flow about circular arc airfoils are discussed and the origin of the oscillations is investigated.

Transonic Flow Phenomena

It will be helpful to distinguish the main features of steady transonic flow in order to organize the discussion of unsteady aerodynamics. Figure 2, from Ref. 4, indicates various regions of transonic flow development for the NLR 7301 airfoil, a 16-percent cambered supercritical-type section. With increasing Mach number and moderate angle-of-attack, the upper surface becomes critical between M = 0.4-0.7 with the first shock forming at an increase of approximately 0.1 in Mach number. Pearcy et al.[55] have classified several types of flow separation which may occur. For conventional airfoils the typical pattern, termed type A, involves the growth of a local separation bubble induced by boundary layer separation at the shock foot, spreading rapidly to the trailing edge as Mach number increases. This condition is often accompanied by unsteady phenomena such as buffet and aileron buzz[4]. The steep aft pressure gradients of modern airfoils, such as the NLR 7301, can lead to an alternate pattern, termed type B, in which separation progresses from the trailing edge towards the shock. Figure 2 illustrates this type B separation, with fully separated flow aft of the shock occuring along the line of maximum lift. Note the small "shock free" design condition occuring over a small isolated range of lift coefficient and Mach number just prior to the onset of trailing edge separation. Tijdeman[4] notes that flow conditions in the region between the onset of trailing edge separation and fully separated flow are very sensitive to Reynolds number and the location of transition from laminar to turbulent flow.

Figure 3 shows a similar diagram, derived from Ref. 56, of flow regions for a complete vehicle. Flows which are predominantly attached or separated are designated as type I and III flows respectively, while mixed attached and separated flows are designated type II. These

flow regions will be used to distinguish the relative difficulty of computational problems. For unsteady flows the boundaries between these flow types are not distinct since an airfoil or wing may exhibit more than one type of flow during the unsteady motion. The "picket fence" in the mixed flow region has been added to emphasize the possibility of "nonclassical" aeroelastic effects in this region. Classical linear aeroelastic analysis methods cannot reliably model results in this region although they have been surprisingly durable.

Farmer et al.[57] provided early test results documenting the effect of airfoil shape upon flutter boundaries. Figure 4 shows their comparison of flutter boundaries for two structurally and geometrically similar wings of the same planform. The supercritical wing was a reduced stiffness model of the modified TF-8A wing while the conventional wing had a symmetrical section. The two wings had leading-edge sweep angles of 44.5 degrees. Design cruise Mach number was 0.90 for the conventional wing and 0.99 for the supercritical wing. The supercritical wing was shown to have a 25 percent lower minimum flutter dynamic pressure near Mach 1.0 where type II mixed flow would be expected. Current transonic computational methods are beginning to address this important area which will be a key topic for computational aeroelasticity in the future. Other reports of aeroelastic model tests relevant to this area are; single mode flutter of a low aspect ratio wing studied by Erickson[58], supercritical wing flutter tests performed at the NLR[59,60] and torsional buzz of aeroelastic wings tested at the RAE[61]. It should be noted that the present paper deals only with the computational methods for predicting the type A and B flow separations. Separated flows involving 3-D unsteady vortex flow structures are also of great importance in this field but are outside the scope of this paper.

Experimental Data Sets

In this section, the airfoil geometries and wing planforms which have been most frequently studied are summarized. In addition to the AGARD standard configurations, several other model tests have been popular for comparison with computational results. Figures 5 and 6 show the profiles and planforms of the 2-D[6] and 3-D[9] AGARD configurations, respectively. Data sets for all of these configurations except the 6 percent parabolic arc, DO A1 and MBB-A3 airfoils are given in Refs. 10, 11, and 70. Tables 1 and 2 tabulate selected references for these and other configurations in which comparisons of experimental and calculated unsteady pressures are given. The entries are grouped by the equation level of the physical modeling used for the calculations. The references are not exhaustive but are an attempt to indicate publication of significant experimental/computational comparisons or new capability.

The first three airfoils in Table 1 are conventional airfoils with 6, 10, and 12 percent thickness ratios. Tijdeman[4] tested the NACA 64A006 airfoil with an oscillating quarter-chord trailing-edge control surface. Interpretations of these tests[4] have provided insights into the underlying mechanisms of unsteady transonic flows. Tijdeman indentified three types of shock motion, denoted type A, B, and C. In type A shock motion, the shock wave remains distinct during the oscillation cycle, with a periodic variation of shock location and shock strength. In type B shock motion, the shock wave weakens and disappears during a portion of the cycle, generally during the forward propagation of the shock along the surface. For type C motion, the shock wave on the airfoil remains distinct and propagates forward along the airfoil chord and off the airfoil leading-edge.

Davis and Malcolm[62] tested the NACA 64A010A airfoil for pitching oscillations. Two cases from this test have been widely studied: a case with a moderate shock wave at $M = 0.8$ and $\alpha = 0$ degrees and a case with steady shock-induced separation at $M = 0.8$ and $\alpha = 4$ degrees. The NACA 0012 airfoil, tested by Landon[10], differs from the other entries in Table 1 in that it was tested for larger dynamic pitching amplitudes and for transient ramping motions making it suitable for dynamic stall computational studies. McDevitt and Okuno[63] have reported measurements of periodic shock-induced oscillations for this airfoil.

Data sets for the 16 percent thick supercritical NLR 7301 airfoil are given by both Tijdeman and Davis[10] and the shock-free condition for this supercritical airfoil has been a challenging computational case. The 8.9 percent thick MBB A-3 airfoil has been tested by Zimmerman[64] and represents a less severe supercritical airfoil computational case. Other supercritical airfoils tested for oscillatory motions or exhibiting unsteady behavior are: a 12 percent thick airfoil tested for pitching, heaving, and flap rotation by den Boer and Houwink[65], the RA16SC1 airfoil tested by ONERA[66], and the cryogenic test of a supercritical SC(2)-0714 airfoil by Hess et al.[67] Reference 65 reported large dynamic responses of airloads on the supercritical airfoil for both oscillating and static motions at type II flow conditions and introduced the concept of "aerodynamic resonance." Similar periodic shock-induced oscillations are reported for the RA16SC1 airfoil.[66]

Tests of rigid circular arc airfoils have been reported by McDevitt et al.[35], McDevitt[36], Mabey[38] and Mabey et al.[39] References 35 and 36 give details of tests of an 18 percent thick airfoil for Reynolds numbers of 1 million to 17 million, covering laminar to fully developed turbulent flows. The wind tunnel walls were contoured to approximate the inviscid stream-lines over an airfoil at $M = 0.775$. Periodic unsteady airflows were observed over a narrow Mach range whose extent depended upon whether Mach number was increasing or decreasing. Forincreasing Mach numbers, oscillations occurred for $0.76 < M < 0.78$ while for decreasing Mach number the range was wider, $0.73 < M < 0.78$. The frequency of the oscillations was 188 ±3 Hz (reduced frequency $k = 0.48$ based upon semi-chord). Mabey[38] studied similar periodic flows for a series of circular

arc airfoils ranging in thickness from 10 to 20 percent at Reynolds numbers of 0.4-0.6 million. In Ref. 39, further investigations on a larger 14 percent thick biconvex wing at Reynolds numbers of 1-7 million is reported. Two necessary criteria evident from the experimental results for the existence of the periodic unsteady flow are given: thickness/chord ratio greater than 12 percent and local Mach number upstream of the terminal shock wave in the range

$$1.24 < M < 1.40$$

McDevitt[36] identifies the predominant shock motion for the 18 percent thick airfoil as type C whereas Mabey et al.[39] argue that it is type B motion.

The smaller number of entries in Table 2 reflects the situation regarding 3-D testing in that there are fewer experimental data sets widely available and fewer comparisons of experimental and calculated results have been published. Tijdeman[14] tested a model of the F-5 fighter wing including external tanks and stores. This wing has an aspect ratio of 2.98, a taper ratio of 0.31 and a leading edge sweep of 32 degrees. The relatively thin wing section, a modified NACA 64A004.8, has made this a popular computational case since it is well within the capability of TSD codes. Transonic and low supersonic test conditions are available. Of the AGARD Standard Configuration models shown in fig. 6, the NORA model is the most extensively tested. It is a model of the Mirage F-1 horizontal tail which has been tested in four European wind tunnels[9,10].

The AGARD rectangular wing and the RAE Wing A model have symmetric airfoil sections[9,10,12] whereas the ZKP wing and LANN wing have supercritical airfoil sections.[9,11] Additional models tested for oscillatory pitching are the NASA Rectangular Supercritical Wing (RSW) model[68,69] and the RAE AGARD tailplane model.[70] The former had a 12 percent supercritical airfoil section while the latter had a NACA 64A010A section, the same as one of the AGARD 2-D configurations.

Also included in Table 2 are references to several other published comparisons with experimental data. These cases are of interest since the models were aeroelastic and some comparisons of experimental and computed transonic flutter boundaries (or aeroelastic response) are given. Isogai gives comparisons for a high aspect ratio super-critical transport wing in Ref. 26 and for the supercritical wing flutter model of Farmer et al.[57] in Ref. 71. Bennett et al.[72] give static aeroelastic comparisons for an aspect ratio 10.3 supercritical wing which was extensively instrumented for unsteady pressure measurements[73]. Finally, Guruswamy and Goorjian[74] present calculations for a rectangular parabolic arc flutter model.

Computational Methods

A variety of methods is available to address transonic unsteady computations. The choice of an appropriate method calls for assessment of the difficulty of the aerodynamic problem being addressed. One possible classification of level of difficulty is indicated in fig. 3 in which type I problems involve attached flows, type II problems involve mixed flows and type III problems involve fully separated flows. Type I flows include one of the most important aeroelastic analysis conditions, cruise at high dynamic pressure. Classical linear aeroelastic analysis has been primarily focused upon this condition. The transition from type I to type II conditions can be induced by manuevering flight and can occur with little decrease in dynamic pressure. Thus, aeroelastic response and stability of type II flows can be quite important although they only recently have been brought within the range of transonic computational methods. Type III flows occur as larger maneuvers are performed and can involve the onset of vortex flows, buffet and dynamic stall. It must also be recognized that the nature of the airflow may change significantly in going from steady to unsteady conditions. For instance, airflows may exhibit intermittently type I and type II conditions while undergoing structural vibrations induced by atmospheric turbulence or by flutter.

Computational methods available for transonic unsteady aerodynamics include potential equation (both TSD and FP), Euler equation and Navier-Stokes equation solvers. The thin-layer Navier-Stokes (TL-NS) approximation is obtained by neglecting components of the viscous terms in the coordinate direction normal to the body surface. Also, viscous flow capability may be added to the potential and Euler equations by means of interacted boundary layer models.

Issues which have been central to unsteady CFD have been the choice of implicit versus explicit algorithms, the stability of alternative solution algorithms and the treatment of computational grids. Explicit schemes are simple to code and easily vectorizable but are limited in allowable time step by the stability limit imposed by the signal propagation time over the smallest grid cell. Faced with the requirement of maintaining time-accuracy throughout the entire field for aeroelastic computations, this easily leads to excessive computation times, especially for viscous flow calculations where a very fine mesh near the surface is required to resolve the boundary layer. The alternative implicit solution algorithms thus are favored and attention must be given to their relative stability and accuracy characteristics. Grid generation for unsteady problems in which the body boundary moves, such as for an oscillating control surface or an aeroelastic deformation, raises new issues over those involved in steady flows. To maintain accuracy, the body-conforming grid must be realigned with the body at each time step. Schemes for accomplishing this have been studied as well as the necessity of moving the grid at all. When body motions are small with perturbations mainly normal to the surface, imposing boundary conditions on the mean surface location may be an acceptable approximation. Finally, the nature of unsteady calculations means that the solution is not allowed to achieve a steady-state and thus the

dynamic response of numerical calculations on the computational grid is more important. For example, grid cell stretching in the near and far field will affect the computational impedance of the grid for unsteady calculations.

In the sections to follow, the status of transonic unsteady aerodynamics is reviewed. It has been helpful to regard the evolution of this computational capability as following four broad stages:

i.) Early computational demonstrations
ii.) Maturation of computational methods
iii.) Application to realistic configurations
iv.) Type II mixed flow computation

A thread which may be discerned in reviewing this field is the continued evolution of computational methods, with applications and evaluations by comparison with experiment, to successively more difficult cases in order to define the boundaries of validity of the computational method. Thus, for instance, an algorithm which was introduced to treat simple type I attached flow cases is upgraded in capability to enable treatment of more difficult type I cases (closer to the type II boundary in Fig. 3) and possibly even type III cases.

Early Computational Demonstration

Three early computations gave impetus to transonic unsteady CFD: demonstration of type A, B, and C shock motions, calculation of periodic aerodynamic oscillationsabout a rigid airfoil and calculation of the aileron buzz boundary for the P-80 aircraft. All three of these cases involve 2-D computations. A fourth significant early development was the 3-D TSD code described by Borland et al.[20] which was the first time-accurate code designed for the aeroelastic analysis of swept wings.

Computation of Shock Motions

Tijdeman's[4] type A, B, and C shock motions observed for the NACA 64A006 airfoil with oscillating flap were demonstrated computationally by Magnus and Yoshihara[5], Ballhaus and Goorjian[6], and Magnus.[15] Figure 7, from Ref. 6, gives these three calculations from the LTRAN2 TSD code with comparisons of Euler code[5,15] results for type A and B. Magnus[15] gives the corresponding Euler code results for type C shock motion. The computational conditions for these three cases are:

Type	Mach	Reduced frequency	Flap amplitude
A	0.875	0.234	1.0 deg.
B	0.854	0.179	1.0 deg.
C	0.822	0.248	1.5 deg.

These conditions are 0.15 - 0.28 Mach lower than Tijdeman's test conditions, very likely due to wind tunnel wall interference. The Euler code used by Magnus and Yoshihara was a Lax-Wendroff explicit differencing solution algorithm and a Cartesian grid with an embedded fine mesh around the moving shocks was used. The boundary conditions were applied at the mean airfoil position. The LTRAN2 code incorporated the Alternating Direction Implicit (ADI) algorithm for the solution of the low frequency TSD potential equation. The Euler code used 5484 grid points and required 1500 seconds per cycle whereas the LTRAN2 code required 8 seconds (CDC 7600 computer).[6] This significant reduction brought the expense of 2-D unsteady transonic CFD calculations within the reach of many researchers.

Periodic Aerodynamic Oscillations

In order to provide experimental data for validation of viscous flow CFD computer codes, McDevitt et al.[35] conducted tests on a rigid 18 percent thick circular arc airfoil. Figure 8 illustrates the parameters of the experiment which was designed to encounter both trailing-edge and shock-induced separations at high Reynolds numbers within the wind tunnel operating limits. Over a narrow range of Mach number, $0.73 < M < 0.78$, oscillatory flow separation was observed, Fig. 9[37]. McDevitt[36] states that the oscillations involve predominantly type C shock motion with small regions of type A motion near the onset of theperiodic oscillations, fig. 10. The reduced frequency of the oscillations is $k \approx 0.48$ for $\alpha = 0$ degrees and varies little with angle-of-attack.

Levy[37] successfully computed such oscillations for this airfoil using a Navier-Stokes flow solver. Levy's code was a modification of the code of Ref. 75 and uses MacCormack's explicit solution scheme with an algebraic eddy viscosity model. Levy modified the code to simulate the contoured wind tunnel walls. Figure 11 shows steady computed Mach contours for Mach numbers of 0.72 and 0.78, corresponding to trailing-edge and shock-induced separations, respectively, and unsteady flow with oscillatory trailing-edge/shock-induced separation for $M = 0.754$. The reduced frequency of the computed oscillations is 0.40, about 20 percent lower than the measured frequency. Note particularly the lower surface Mach contours of the third frame for $M = 0.754$. The few lines indicate the collapse of the supersonic region for this portion of the cycle. Also note the dimpled nature of these Mach lines under the airfoil surface. These features will be discussed in more detail below.

Subsequent tests on circular arc airfoils of thicknesses from 10 to 20 percent were performed by Mabey[38], obtaining similar periodic oscillations. The Mach number range of the oscillations increases with decreasing thickness as does the oscillation frequency, remaining in the range of $0.4 < k < 0.55$ depending on thickness and wind tunnel wall condition. Mabey et al.[39] and Levy[40] give detailed comparisons of Navier-Stokes calculations with experiment for a 14 percent thick airfoil, reproducing qualitatively the details of the oscillatory flow.

Calculation of Aileron Buzz

Aileron buzz is a one-degree-of-freedom aeroelastic instability, usually of limited amplitude, which may be encountered under conditions of transonic flow. Steger and

Bailey[17] studied such a case for the P-80 aircraft which had been tested in a wind tunnel. They simulated a rigid 2-D wing section strip including a free-floating aileron using a thin-layer Navier-Stokes flow solver. They implemented the Beam-Warming implicit Approximate Factorization (AF) solution algorithm, using an algebraic eddy viscosity turbulence model. A novel treatment of the computational grid was used to follow the aileron motion with a conforming gird. A simple shearing transformation in the coordinate normal to the aileron was used.

Figure 12 shows the limit amplitude "aileron buzz" oscillation which was calculated for M = 0.82, Re = 20 x 10^6 and α = -1. The calculation was initiated with a 4 degree aileron offset. This and other calculations successfully reproduced the experimental buzz boundary. The computed reduced frequency was k = 0.38. The shock motion observed in the calculations was type B, and type II intermittent flow separation is shown in Ref. 17. The code was capable of being run in an inviscid mode (EE mode) and several such calculations were made. Below M = 0.84 the aileron exhibited damped oscillations of about k = 0.36 whereas divergent oscillations (k = 0.39) were calculated at M = 0.84. Hence the tendency to oscillate at a given frequency derives from the inviscid flow equations while the viscosity apparently plays the key role of limiting the amplitude of oscillation.

These calculations were performed on a 76 x 42 grid and required approximately 1.5 sec of CDC 7600 computer time per time step or 460 μs. per grid point per iteration. Non-dimensional time steps of 0.005 - 0.01 were used (based on chord).

Swept-Wing Aeroelastic Analysis

Borland et al.[20] and Borland and Rizzetta[21] describe the development of the XTRAN3S TSD code for aeroelastic analysis of swept wings. Reference 20 describes the extension of the LTRAN2 ADI solution algorithm to three-dimensions for the solution of the 3-D low frequency TSD equation. Several cross derivative terms required explicit treatment yielding a semi-implicit algorithm. Results for an oscillating swept wing are given in Ref. 20. Computations on a 60 x 20 x 40 grid required 3 seconds of CPU time per time step on the CDC 7600 computer (62 μs. per grid point per iteration).

Reference 21 describes the extension of this code to solve the complete TSD equation and its application to coupled structural dynamic - unsteady aerodynamic analysis. Samples of flutter calculations for a rectangular wing are given. Computations on a 60 x 20 x 40 grid required 4 seconds of CPU time per time step on the CDC 7600 computer. Static aeroelastic solutions were obtained with 300-400 steps and dynamic aeroelastic solutions in about 1000 steps with nondimensional time steps of 0.1. It is noted, however, that this time step is case dependent, depending on planform, Mach number, etc. This capability is noteworthy as it is the first complete wing flutter analysis accomplished using a time-accurate transonic computational method.

A comparison of calculations from the XTRAN3S code with experimental data was given by Seidel et al.[76] who performed calculations for pitching oscillations of the NASA Rectangular Supercritical Wing. Figure 13(a) shows steady and unsteady pressure distributions for two span stations at M = 0.7 and α = 2 degrees. For this low transonic condition, the agreement with experiment is good except near the leading edge where grid refinement is probably needed. The unsteady results in fig. 13(b) are in good agreement with experiment over most of the chord. Inboard, there is an improvement in the prediction of the leading edge suction peak over the linear theory RHOIV result. Outboard, there is an underprediction of the leading edge peak and evidence of viscous effects in the phase angle in the aft cove region. Calculations for this RSW model have also been reported in Refs. 25, 34, and 77.

Maturation of Computational Methods

In this section, the further development and application of the computational methods introduced in the last section is described. These developments have typically been introduced in 2-D codes. Hence, the exposition emphasizes 2-D methods with parallel 3-D results interspersed.

Augmentations to Potential Methods

Many researchers have participated in augmenting the capability of unsteady potential codes. These developments have extended the range of applicability of transonic potential codes by improved physical modeling and by improved numerical stability or accuracy.

The low frequency LTRAN2 ADI algorithm was limited in accuracy above k ≈ 0.1 and additions of the neglected time derivative terms are described in Refs. 78-83. Chow and Goorjian[82] describe the addition of high-frequency terms and special treatment of the farfield boundary conditions to account for the physical domain of dependence for supersonic freestream conditions. This enabled calculation of 2-D supersonic results and enhanced the stability of the code. Increased stability was also added to the LTRAN2 code by Goorjian et al.[84] with the replacement of the Murman-Cole differencing method by the monotone differencing method of Engquist and Osher.[85] This method eliminates the nonphysical formation of expansion shocks in the leading-edge region and allowed a large increase in allowable time step size.

The far-field boundary conditions imposed can have special significance for unsteady calculations since disturbances emanating from these boundaries may return to the vicinity of the airfoil and contaminate the solution. Kwak[86] implemented non-reflecting boundary conditions in the LTRAN2 code and showed that the computational grid could be made smaller with reduced computer costs. Whitlow[87]

implemented similar conditions for the complete TSD potential equation. Reflections from internal grid points can also occur if the grid stretching is excessive. Seidel et al.[76] show results indicating that grid stretching in the direction normal to the airfoi is most critical.

The XTRAN2L TSD code described by Whitlow[87] incorporates the features mentioned above and typical results from this code are shown in figs. 14 and 15 for the NACA 64A010A airfoil. Figure 14 shows the steady pressure distribution for the moderate shock case of Davis and Malcolm while fig. 15 compares the unsteady lift coefficient with experiment and the LTRAN2-NLR and LTRANV (with interacted viscous effects) results of Houwink.[88] Agreement is good for moderate frequencies while there is a characteristic overprediction of the imaginary part for the lowest frequencies. Similar comparisons for a number of the 2-D AGARD configurations are given in Refs. 89-93.

Batina[94] studied the effect of airfoil shape, thickness, camber, and angle-of-attack upon unsteady airloads using the XTRAN2L code. An interesting feature shown in Ref. 94 is illustrated in fig. 14(a) which shows frequency response functions of pitching moment due to a pulsed airfoil pitching motion for three different airfoils. Fourier transform analysis of such motions and airloads has been shown to be very useful in transonic unsteady aerodynamic calculations[76], notwithstanding the nonlinear nature of the flow equation. Note the "hump" in the real part and the coincident "wave" of the imaginary part of the pitching moment curves near k = 0.6. Such resonance features are familiar to dynamicists as similar to the response of damped mechanical oscillatory systems. Examples from Ref. 94 show that the frequency and strength of this resonance feature are primarily a function of Mach number with airfoil shape and thickness being secondary effects.

Berry et al.[95] show a similar resonance near k ≈ 0.25 in the pitching moment due to flap deflection for the NACA 64A006 airfoil at M = 0.85. New calculations for this airfoil are shown in fig. 17 for M = 0.822 and 0.854. These are the conditions shown in fig. 7 for type B and type C shock motion. The symbols in fig. 17 give the complex valued pitching moment coefficients for these two cases derived from separate harmonic oscillation calculations. Note that the type B shock motion (which is reproduced by the XTRAN2L code) was observed near the "resonance" frequency at k ≈ 0.2 for M = 0.854 whereas the type C shock motion is observed at a frequency approximately one-half the resonance frequency at M = 0.822. This resonance-type structure is not observed in the pitching moment frequency response function for M = 0.875 (type A shock motion) where a strong shock has formed.

Nonunique Solutions of the Potential Equation

Steinhoff and Jameson[96] have demonstrated that the potential equation for transonic flow can have nonunique solutions due to entropy generation within shocks violating the isentropic assumption upon which the theory is based. Williams et al.[97] have studied this effect for the TSD equation. Figure 18 illustrates the multiple solutions obtained for the NACA 0012 airfoil at M = 0.85. The unsteady results given on the right of the figure (k ≠ 0) demonstrate that large phase errors may occur at low reduced frequencies as the solution jumps between the stable equilibrium solutions at A and C. Fuglsang and Williams[98] have developed modifications to the TSD equation to circumvent this problem. These nonisentropic modifications involve a modified flux term, a correction to the pressure coefficient equation and a correction to the wake jump condition to allow entropy convection. These modifications correct the multiple solutions and enable the use of the TSD equation for a wider range of problems. Nonisentropic cases studied by Fuglsang are noted in Table 1. Gibbons et al.[99] extended this method to 3-D using the XTRAN3S TSD code and found evidence of similar multiple solutions. Figure 19 shows time histories of lift coefficient following a pitch pulse excitation. For aspect ratios greater than 24 the lift diverges to a non-zero steady state. Gibbons implemented the 2-D modifications discussed above stripwise in the XTRAN3S code, obtaining the results in fig. 20. The unmodified code predicts a lift curve slope which is twice as large as that obtained with an Euler code whereas the modified code agrees with the Euler code result. Gibbons also shows results for the RAE AGARD tailplane model where the nonisentropic modifications resulted in a foward shift of the shock near the wingtip of nearly 10 percent chord. Further studies of this effect are needed to give a complete assessment of this effect for potential codes. Finally, Osher et al.[100] and Whitlow et al.[101] have also developed entropy condition satisfying approximations for the unsteady FP equation.

Treatment of Moving Grids

For solution of flow equations above the TSD level, body conforming grids are generally used. For aeroelastic applications in which the structural boundary moves from iteration to iteration, the issue of redefining the grid at each step must be addressed. Generally, the problem of grid definition is of such difficulty that approximate methods have been sought. Chyu and his coworkers[18,19] used an interpolation scheme for defining grids at intermediate steps between the extremes of motion for oscillating airfoils. They used Steger's[102] Navier-Stokes code to study the moderate shock case[18] and the shock-induced separation case[19] for the NACA 64A010A airfoil, shown in figs. 21, 22. Note that the full and thin-layer Navier-Stokes results in fig. 21 show no differences except near the shock. This is an important demonstration of capability for type II-III flows with intermittent separation. These calculations were obtained using 2620 steps per cycle of oscillation and the time per step on the CRAY X-MP computer was: 0.33 sec, full NS; 0.22 sec, TL-NS; 0.17 sec, EE, correspoinding to 25-44 μs. per grid point per time step.

If the surface motion is small and primarily in the direction normal to the x-axis, a suitable engineering approach may be to apply the boundary conditions at the mean surface location with suitable terms added to the boundary condition to simulate surface motion. Sankar et al.[103] have made a preliminary evaluation of this method for unsteady calculations using 2-D and 3-D FP codes. For the 2-D code, a case with an oscillating trailing-edge flap with one degree amplitude was studied. They find that results using the exact boundary conditions with a moving grid and the transpiration approach differed by no more than 10 percent for surface pressures and integrated loads. Further studies are required before the viability of this transpiration boundary condition method can be assessed.

Interactive Viscous Modeling

Within the range of type I unsteady aerodynamic problems, fig. 3, viscous effects become more important with increasing lift coefficient or Mach number. Further increases lead to the development of type II mixed attached and separated flow where viscous effects must be addressed. This borderline region between type I and type II flow is important since design operating conditions frequently occur here. Thus simplified methods of accounting for viscous effects without resorting to NS codes have been sought. These interacted boundary layer methods have most frequently coupled an inviscid potential flow outer region solver with an integral boundary layer equation inner region viscous flow solver. The two solutions are coupled iteratively through the boundary conditions to ensure consistent coupling. In the "direct" coupling method, the inviscid flow solution provides the pressure coefficient at the edge of the boundary layer, enabling a direct solution for the boundary layer displacement thickness. This thickness distribution is then added to the airfoil geometry to provide the boundary condition for the next iteration of the inviscid solution. For separated flows, it is necessary to invoke an "inverse" boundary layer method wherein the displacement thickness is specified and the edge pressure coefficient calculated. Consistency of the inner and outer solutions is maintained by iterating the solution at each step.

Couston et al.[104] published unsteady interacted solutions using a TSD potential code[105] and a viscous defect formulation of the boundary layer equations. Results for attached flows for the NACA 64A006 airfoil are given. In subsequent calculatons, LeBalleur and coworkers, in Refs. 66 and 106-108, have pursued this technique for a wide range of attached and separated flow cases. Cases of airfoils with slats and flaps and airfoils with spoilers are treated. Also, cases of periodic oscillations on the 18 percent biconvex airfoil[66,109] and the RA16SC1 supercritical airfoil[66] are described.

Similar interacted viscous solutions are given by Houwink[88,110] and by Rizzetta[111]. Applications of Rizzetta's method are given in Refs. 95 and 112-115. Ruo et al.[77] show 3-D calculations using 2-D strip and 3-D integral boundary layer methods with a FP inviscid code. The viscous defect formulation used by LeBalleur retains time-accuracy for the boundary layer equations whereas Houwink and Rizzetta's methods use a quasi-steady (i.e. time-independent) boundary layer. A comprehensive assessment of flow conditions requiring time-accurate viscous effects would be a valuable addition to the field. Tables 1 and 2 note references in which interacted viscous modeling has been used in comparisons with experimental data.

Solution Algorithms

Advances in solution algorithms for unsteady CFD have been made for all levels of physical flow modeling. Sides[30] summarizes work aimed at making time-accurate Euler equation solutions more efficient using an explicit predictor-implicit corrector algorithm. Artificial viscosity is added only in regions of high gradients and stable solutions for a Courant number of 12 are shown. Results for the NLR 7301 airfoil at its design "shock-free" condition, $M = 0.721$ and $\alpha = -0.19$ degrees, are given in figures 23-25. Figure 23 compares calculations from the Euler code and a hodograph method with experimental data. The computational conditions differ from the test conditions due to wind tunnel corrections and boundary layer effects[10]. The two calculations agree well except for a weak shock in the Euler solution. It is noted that the Euler solutions were very sensitive to small changes in either Mach number or angle-of-attack about this condition. Figure 24 shows the steady isobar lines about this airfoil calculated by the Euler code. Note the nearly horizontal isobar pattern shown in the supersonic region over the top of the airfoil. Results are presented for flap oscillations at a reduced frequency of $k = 0.068$ and fig. 25 shows instantaneous isobar patterns for $\omega t = 0$ degrees and 180 degrees. Note the dimpled isobar pattern on the upper surface for $\omega t = 0$ degrees. Very good agreement of computed and measured unsteady pressures is shown in Ref. 30 for this case. These calculations were performed on a 188x24 grid and required 2180 steps per cycle, using 315 sec per cycle on a CRAY 1S computer, corresponding to 32 μs. per grid point per time step. A factor of 10 increase in speed over the explicit method was achieved with this semi-implicit method.

Another semi-implicit solution algorithm isdescribed by Isogai[26] for the FP equation. The USTF3 code solves the nonconservative 3-D FP equation and also implements a quasi-steady 2-D strip viscous boundary layer method. Several results for the AGARD standard wings are shown and significant aeroelastic flutter calculations are compared to experimental flutter results which will be discussed later.

The semi-implicit ADI solution algorithm used in the XTRAN3S TSD code required increasingly small time steps to maintain stability as wing sweep and/or taper was increased. Guruswamy and Goorjian[116] replaced the grid shearing transformation of the code with a modified shearing transformation which

mapped from a rectangular physical domain onto a rectangular computational domain. This alleviated the stability problem, allowing time steps of 0.01 for the F-5 wing model whereas time steps an order of magnitude smaller had been marginal with the original method. Figures 26 and 27 show the steady and unsteady pressures calculated for this aspect ratio 2.98 wing. The leading edge sweep angle is 32 degrees and 1200 steps per cycle were used. Both steady and unsteady computations agree closely with experimental results and are representative of other applications of both TSD and FP codes listed in Table 2.

Two advances in solution algorithms for the unsteady FP equation are reviewed next. The first was the development by Malone and Sankar[117] of a strongly implicit AF scheme for the 2-D conservative potential equation using body fitted coordinates. Upwind density biasing is used for stability in supersonic zones. Results from the 2-D SUNTANS code are given in Refs. 117 and 118 for several of the AGARD 2-D configurations. Malone et al.[24] have also developed a 3-D version of the strongly implicit AF algorithm and published comparisons of unsteady pressures with data for the F-5 wing model[24], the LANN wing model[77] and the NASA RSW model[77]. Figures 28 and 29 show steady and unsteady pressures at two span stations for the F-5[24] at M = 0.95. The agreement with experiment is quite good. This USIPWING code is implemented on the VAX 11/780 computer. Three-dimensional unsteady results are typically obtained with 240 steps per cycle using nondimensional time steps of 0.03-0.06.

The second FP algorithm development to be noted was the development of the flux-biased AF method by Osher, Hafez, and Whitlow, Refs. 100, 101, and 119. The method satisfies an entropy inequality ruling out expansion shocks and accurately tracks sonic conditions, requiring no empirical constants to specify the amount of artifical viscosity needed for stability. Whitlow et al.[101] gives details of the method implemented in a 2-D FP code and show examples for the NACA 0012 airfoil. Shankar et al.[120] and Shankar and Ide[25] have used the flux-biased AF technique in a Newton linearization method with internal iterations to reduce the linearization and factorization errors and efficiently treat unsteady flows with large time steps. Reference 120 presents results for the NACA 0012 airfoil for nondimensional time steps of 0.1, 0.2, and 0.3 (corresponding to CFL numbers of 35, 70, and 105). The number of internal iterations is increased with the larger time steps to maintain accuracy. For unsteady calculations with two internal iterations the 2-D code required 0.09 seconds per iteration on a CRAY X-MP computer with a 181x30 grid, corresponding to 16 μs. per grid point per time step. In Ref. 25 an extension of this flux-biased AF method to 3-D is described. Sample calculations for the NASA RSW model are given and excellent stability characteristics are quoted. On a 100x16x20 grid, calculations were obtained for 100 time steps per cycle (Courant numbers greater than 100) in about 60 seconds on a CRAY X-MP computer, corresponding to 18 μs. per grid point per time step.

Batina[23] has implemented a 3-D AF algorithm for the TSD potential equation which is similar to Shankar's[120] method in using a Newton linearization in time coupled with internal iterations. Results for the F-5 wing model at M = 0.9 were calculated for 100, 200, 300, and 400 steps per cycle. The results for 100 steps per cycle indicated that the time step was too large for engineering accuracy. Comparison calculations with the XTRAN3S ADI algorithm required 2000 steps per cycle. An advantage of such an efficient 3-D TSD code is that body conforming grids are not required and codes may be configured to treat complex geometries. Of course, this advantage must be balanced against the loss of some physical modeling fidelity with the small disturbance approximation. It seems certain that a variety of unsteady computational methods, with a range of physical modeling approximations, will eventually be used within the design process.

The time-dependent Euler equations form a hyperbolic system of equations, and much of the recent progress in algorithm development[121-126] has hinged upon the incorporation of the signal propagation features of the differential equation into the numerical algorithm. There are several methods of incorporating this information into a difference scheme, for example flux-vector-splitting or flux- difference-splitting, and an excellent review of the current developments in the field is given by Roe in Ref. 127. The advantages of incorporating an upwind-biased discretization into a numerical algorithm are twofold: (1) the scheme becomes naturally dissipative so that no adjustable constants need to be fine-tuned to a particular application and (2) improved implicit schemes can be devised for more efficient solutions to both steady and time-dependent problems. Both of these advantages offset the disadvantage that approximately twice as many operations per time step are required to implement an upwind scheme as opposed to a central difference scheme.

Most of the calculations made to date with upwind difference schemes, especially for airfoils/wings, have been steady-state applications, for which comparable accuracy can be obtained by central difference methods with added artificial viscosity. The advantages of upwind differencing should be more significant for time-dependent problems, however, where the ability to treat rapid movement of flows with shocks is required. Roe[127] gives several examples of shock-propagation computations in two-dimensions which demonstrate clearly the advantages of a characteristic-based scheme. Viscous effects can also be readily introduced into upwind difference schemes developed for the Euler equations by central differencing the shear stress/heat transfer terms[128,129].

The time-accurate computations made by Steger and Bailey[17] and Chyu et al.[18,19] used a spatially-split approximate-factorization (ADI) scheme, which is unconditonally stable in two dimensions but at most conditionally stable in three dimensions. Alternate factorizations are possible with the incorporation of an upwind difference discretization in one or more coordinate directions which can lead to

unconditionally stable 3-D algorithms[121]. A two-factor eigenvalue-split scheme for the Euler equations has an increased stability limit and fewer operations than the spatially-split scheme, although the operations are not completely vectorizable. Belk[34] computed steady and time-dependent inviscid flows for the NASA RSW model with such an algorithm in combination with a blocked-grid strategy. Ying et al.[130] used upwind differences in a single coordinate direction and constructed a two-factor unconditionally stable algorithm for which thin-layer viscous effects are readily incorporated. Applications of the thin-layer Navier-Stokes equations to the high-angle-of-attack unsteady flow over a hemisphere-cylinder are made[130]. Several of these alternate factorizations are investigated in the context of efficient algorithms for three-dimensional steady-state problems by Anderson et al.[131,132].

The use of multigrid techniques to accelerate convergence to the steady-state is becoming widespread in the aerodynamic community. These techniques can also be used for time-dependent flows. For instance, multigrid techniques could be used to efficiently solve the large banded matrix equations arising from implicit time discretizations, the solution of which is generally approximated through relaxation and/or factorization methods. Jesperson[133] has demonstrated a time-accurate multiple grid procedure which was used to overcome the small time step limitation of an explicit scheme. With the growing memory of today's computers (the Numerical Aerodynamic Simulator has 256 million words of memory) it becomes feasible to solve the banded matrices by direct Gaussian elimination, rather than by approximate techniques. The structure of future implicit algorithms for both steady and time-dependent problems will likely involve a multiple grid algorithm with direct elimination techniques used on the coarser grid levels.

Treatment of Realistic Configurations

All results presented thus far have dealt with unsteady transonic aerodynamics for isolated lifting surfaces. In order to realize necessary improvements over existing aeroelastic analysis methods, computational aeroelastic analysis will be required to provide reliable predictions for complex configurations. Capability to treat such details as wing-fuselage interference, and wing-pylon-store effects upon flutter boundaries are needed. It is encouraging that studies directed at building the capability of treating these more realistic configuration details are progressing.

Batina has added to the XTRAN3S code separate capabilities for treating interfering lifting surfaces[134] and fuselage-wing combinations[135]. The first study is a direct extesion of the ADI algorithm to treat two lifting surfaces. Figure 30[134] illustrates a case of canard-wing interference in which unsteady loads are induced on the wing by the oscillating canard. This effect is obviously a function of the separation distance between the surfaces and the Mach number and frequency. Shankar and Goebel[136] have also published a treatment of canard/wing modeling for the unsteady full potential equation. Steady results are shown for a canard/wing research model and the HIMAT vehicle but no unsteady results are given. Batina[135] describes the treatment of the fuselage which was implemented in the XTRAN3S code. Boundary conditions are applied upon a computational fuselage surface aligned with coordinate lines and are formulated in terms of projected areas and arclengths of the true fuselage. Comparisons with existing steady data are favorable. Figure 31 shows the calculated interference effect of the RAE wing/fuselage model for an assumed wing bending mode. The interference effect on the integrated generalized force, important for aeroelastic analysis, is approximately 5 percent of the total. Malone and Sankar[137] have also addressed the treatment of wing-fuselage modeling. They used a body fitted coordinate system with the USIPWING code and present comparisons with steady data from a research transport wing, the F-14 airplane and a RAE Wing/Fuselage model. While unsteady results are shown, there are no experimental data for comparison.

Heavy, concentrated masses such as engines, stores, and tanks can have a large effect upon flutter boundaries and sometimes placement of these components is critical to meeting design objectives. Guruswamy et al.[138] have augmented the ATRAN3S code to treat a wing with a tip store. The store is modeled within the TSD approximation by treating the tip store as an extension of the wing planform. Comparisons with data from the F-5 wing model with a tip store[14] are presented.

Thus, a promising start has been made in the treatment of realistic configurations. The trend to be observed in these examples is that capability for an additional component has been added to existing codes which treat isolated wings. Based on the recent progress in devising steady flow solution methodology for complex configurations, one might anticipate the development of codes aimed "ab initio" at more complete configurations in the near future. Another evident requirement is for the necessary experimental data to validate codes for such configuration details. Such tests are quite expensive and require much time for planning and execution. In the meantime, careful attention to comparisons with available steady data is a necessary starting point in any case.

Aeroelastic Applications

The major intended use of unsteady aerodynamic calculations is for prediction of aeroelastic response of aircraft and, more specifically, flutter. This section will review, very briefly, the available publications. There have been numerous published calculations of two and three degree-of-freedom 2-D flutter studies which are devoid of experimental data comparisons since realistic 2-D flutter models are very difficult to fabricate. On the other hand, there are only a small number of published 3-D flutter calculations which are compared with

experimental results. An important reason for this is the detail and effort requred to perform a valid flutter analysis of a flutter model. Vibration mode shapes and masses must be accurately calculated or measured and surface coordinates measured. Another major factor has been the difficulty of the unsteady aerodynamic computation for configurations of current interest. For instance, much interest tends to be focused upon cases whose transonic flutter boundaries occur coincidentally with the onset of mixed flow. Hence, aeroelastic applications for such cases has had to await the maturation of computational methods discussed above.

A restricted selection of the many publications of 2-D flutter calculations includes Isogai[80], Edwards et al.[139], Bland and Edwards[83], and Berry et al.[95]. References 80, 83, and 139 document the somewhat surprising "locally linear" nature of transonic potential flows. That is, about the steady mean flow condition which is a nonlinear function of Mach number and angle-of-attack, unsteady perturbation airloads behave very linearly for reasonable airfoil motions. Figure 32[83] illustrates this by showing the normalized unsteady lifting pressure on the NACA 64A010A airfoil for oscillatory pitch amplitudes from 0.25-2.0 degrees. Away from the shock pulse little effect of amplitude is seen while the integrated effect of the shock pulse also varies only slightly. Reference 139 introduced the static twisting of the airfoil due to the steady pitching moment into the flutter problem and demonstrated a marked effect upon flutter boundaries, particularly for the supercritical MBB A-3 airfoil. Reference 95 documented the utility of s-plane Pade' curve fits of transonic airloads (which rely on the concepts of linearity and superposition) for aeroelastic analysis. Viscous effects are shown to generally result in larger values of flutter speed since transonic effects are alleviated by the boundary layer.

Comparisons of calculated and experimental flutter boundaries for wings have been given by Guruswamy and Goorjian[140], Isogai[26,71], and Myers et al.[141]. Reference 140 gives comparisons for a rectangular wing flutter model using an early low frequency version of the XTRAN3S code. Reasonable agreement of flutter speeds is shown at a subcritical speed, M = 0.715, but the flutter speed is overpredicted by 75 percent at M = 0.9. Isogai[71] studied the supercritical wing of Farmer et al.[57] using the nonconserva-tive FP USTF3 code and an interacted boundary layer model. His comparison of flutter boundaries is shown in fig. 33. The trend of the transonic flutter dip is very nicely predicted although the dip occurs about 0.08 low in Mach number. The subcritical flutter boundary is very well matched by the calculated flutter point at M = 0.8. The premature flutter dip and the subsequent premature rise of the calculated boundary is of concern since Myers[141], presenting XTRAN3S calculations for a transport wing, also shows such a premature rise in the boundary. Finally, Isogai[26] shows flutter comparisons for a different super-critical transport wing which agree nicely with the experimental flutter dip.

Since the definition of these minimum flutter speeds very likely involves type II mixed flow, it is not surprising that few calculations are available. It can be anticipated that with the recent advances in computational algorithms and interactive viscous modeling, such cases will be treated in the near future.

Type II Mixed Flow Computation

As indicated above, the unsteady periodic flows encountered over a limited range of Mach number and triggered by oscillating trailing-edge/shock-induced boundary layer separation are just recently coming into the range of computational methods. The weakest link for this capability is the uncertainty in the turbulence modeling of complex separated flows, since rapid progress continues to be made in the development of improved algorithms and faster computers.

It is well known that separated flows depart strongly from equilibrium - type behavior, so that at a minimum some account of the non-equilibrium "upstream history" effects should be included in the computations. Some encouraging results along this line have been obtained by LeBalleur[109] with an integral boundary layer model and Johnson[142] with an eddy-viscosity Reynolds-shear stress closure model. Simpson[143] recently reviewed calculation methods for turbulent separated flows and Coakley[144] compared several methods for airfoil applications.

On the other hand, Levy[37] was able to reproduce the unsteady periodic flow behavior of the 18 percent circular-arc airfoil using an equilibrium two-layer algebraic model. The steady flow at Mach numbers below the range of periodic flow, characterized by trailing-edge separation, was predicted accurately. Levy demonstrated that the influence of the channel walls had a substantial impact on the comparisons with experiment, especially at Mach numbers away from the design point. This effect was not considered in the earlier comparisons of Deiwert[75] with the experimental results. The steady flow at a Mach number above the range of periodic flow, characterized by shock-induced separation, was not accurately predicted, as the calculation demonstrated a normal shock pattern (fig. 11) with trailing-edge pressure recovery, whereas the experiment indicated an oblique shock pattern and a constant pressure region downstream of the shock. Coakley[145] domonstrated that the discrepancy was partly attributable to the turbulence model but more so to the blockage introduced downstream by the separated wake flow, which forces the downstream static pressure to be lower than the upstream static pressure. By modeling the tunnel walls with boundary conditions more appropriate for an internal flow and using a modified two-equation turbulence model, Coakley[145,147] obtained good agreement with the steady experimental results, as shown in fig. 34. The above discussion illustrates some of the difficulties which can be encountered in applying and validating computational methods for turbulent separated flows.

In addition to Levy's calculations, the unsteady periodic behavior for the 18-percent biconvex airfoil has also been computed by Steger[102] and by LeBalleur[109]. Steger's calculation was for an airfoil in free-air with an implicit Navier-Stokes code using the Baldwin-Lomax[146] algebraic model. The unsteady flow occurred at a higher Mach number (M = 0.783) than that of Levy (M = 0.754), which can partly be attributed to the free-air boundary conditions. The computed reduced frequency (0.41) was remarkably close to that of Levy (0.40) although both are low in comparison to experiment (0.48). LeBalleur's recent calculations were also made in free-air with a small disturbance potential method including an interacted two-equation integral viscous model. Steady shock-induced separation was computed at M = 0.788 and unsteady periodic flow at M = 0.76. The reduced frequency (0.34) was lower than either of the two Navier-Stokes solutions.

Some calculations have been made during the preparation of this paper using the implicit upwind-biased Navier-Stokes algorithm described in Ref. 149 using an algebraic turbulence model[146]. The tunnel walls were modeled and boundary conditions appropriate for internal flow were used, i.e., the downstream pressure and upstream enthalpy, entropy, and flow direction were specified. The results indicated unsteady flow at a higher Mach number than Levy; steady trailing-edge separation occurred at M = 0.754 and unsteady periodic flow at M = 0.78, although the Mach number for onset of the unsteadiness was sensitive to whether or not the divergence of the tunnel boundary to account for boundary layer growth was included. Figure 35 shows Mach contours through one half-cycle of oscillation (near maximum lift to minimum lift) indicating the forward movement, disappearance, and subsequent formation near the trailing edge of the lower surface shock. The reduced frequency of the type B unsteady motion was 0.406, in close agreement with the calculations of both Levy (compare fig. 11) and Steger. The implicit calculations were made with a time step of 0.01 and a computational time of 18 μs. per grid point per time step on the CYBER 205 computer.

The unsteady periodic flow for the 18 percent circular arc is triggered by the oscillating trailing-edge/shock-induced boundary layer separation on the airfoil. The unsteady motion can also occur in purely inviscid flows because of the vorticity introduced at a curved shock. The flow past a circular cylinder at M = 0.5 is well known, for example, to be unsteady[148,150] exhibiting a type B oscillatory shock motion at a reduced frequency of 0.50. Barton and Pulliam[151] have also shown for airfoils at high-angle-of-attack that the curved shocks near the leading can lead to shock-induced vorticity and periodic self-induced oscillatory flow. To what extent the inviscid mechanism is playing a role in the unsteady circular arc cases is not known, and a parametric study in terms of thickness and Mach number to establish the range of the inviscid mechanism would be very informative.

The calculation of the unsteady periodic flow boundaries for airfoils is a fruitful area for the development and validation of computational methods. Experimental pressure data[35,36,38,39] over a wide range of Reynolds number is available, although detailedboundary-layer measurements are not. For the 18-percent biconvex experiments of McDevitt, a substantial hysteresis effect in the unsteady flow boundary was found. This aspect has not been demonstrated with computational methods as yet, but it would be expected, based on the above discussion, that computational modeling as close as possible to that of the experimental conditions will be a critical consideration. The most interesting behavior, and the most challenging from the computational viewpont, occurs in the transitional region from laminar to turbulent flow. In the experiment of McDevitt[35], the Mach number range for the observed unsteady flow diminished near a Reynolds number of 3×10^6 (fig. 9) and in the experiments of Mabey[39], it disappeared completely in the range of Reynolds number from about 3×10^6 to 5×10^6. Scale effects in either experiment were not significant once turbulent flow is fully established ahead of the shock.

The frequency of these oscillations is of interest in that the flow mechanism causing the unsteadiness might be identified via the characteristic time constants of signal propagation within the various flow regions. Tijdeman[4] noted an almost linear relation between the phase lag of the shock motion and the airfoil motion for type A shock motion with a well-developed shock (for pitch oscillations of the NLR 7301 airfoil). He related this to the signal propagation time from the trailing-edge to the shock. Mabey[39], commenting on characteristic time constants for the 14 percent circular arc airfoil periodic oscillations, notes that this reasoning leads to reduced frequency parameters of 1.15 to 1.8, much higher than the observed frequencies.

Three items mentioned above germane to this discussion are; Steger and Bailey's[17] inviscid EE calculations for the aileron buzz case, LeBalleur and Gerodroux-Lavigne's[109] interacted viscous-TSD code resultfor periodic oscillations, and Batina's[94] demonstration of the possibility of aerodynamic resonance with an inviscid TSD code. The occurrence of damped and undamped oscillations observed for inviscid flows at nearly the same frequency as the oscillations in viscous flow[17] ($k \approx 0.36$-0.39) implies that the flow mechanism determining the oscillation frequency derives from the dynamics of the inviscid flow region. Furthermore, the results of Refs. 94 and 109 give impetus to studying this effect with a TSD code. Accordingly, calculations were made with the XTRAN2L code of the aerodynamic response for the 18 percent thick circular arc airfoil due to trailing-edge 25 percent chord flap motions. The nonisentropic modifications described in Ref. 98 were used to obtain solutions for this strong-shock case. Figure 36 presents the resulting $c_{m\delta}$ frequency response function for Mach numbers of 0.66-0.74. There is a very marked development of an aerodynamic resonance effect as Mach number increases. For M = 0.74 the airfoil resonance frequency is k = 0.32, very close to the computational conditions of

Ref. 109 for periodic oscillations (M = 0.76 and k = 0.36). Steady calculated flow conditions for this case gave a shock location at x/c ≈ 0.73 with a preshock minimum pressure coefficient of C_p = -1.27 (the experimental values were x/c ≈ 0.65 and C_p = 1.1[36]). Although this case is certainly outside the bounds of a TSD code, the occurrence of such a strong resonance feature as shown in fig. 36 is of interest. Experimental evidence of such aerodynamic resonances is given by den Boer and Houwink[65] who tested a 12 percent thick super-critical airfoil. For pitching oscillations, a large resonance effect was observed near k ≈ 0.25 at conditions corresponding to onset of type II mixed flow.

The calculations of fig. 36 were obtained using a 1 degree flap pulse. For the tests of Ref. 36, the inclination angle of the shock-separated region to the airfoil surface ranged up to 7 degrees. Thus, harmonic oscillation calculations for this condition with a flap oscillation amplitude of 7 degrees (not shown) were made which show the development of the characteristic dimpled isobar pattern seen in the NS code results of fig. 35, sketch C. These dimpled isobar patterns have been noted in Levy's[37] NS calculations (fig. 11), Sides EE calculations[30] (fig. 25) and the present NS calculations (fig. 35) and appear to be a variant of type B and type C shock motions. That is, during a portion of the oscillation two regions of high suction pressure occur simitaneously. The dynamic behavior of the boundaries of these regions (i.e. moving shocks and pressure waves) is an interesting topic for further study.

Concluding Remarks

We have attempted to summarize the status of computational methods for transonic unsteady aerodynamics with a focus upon methods for aeroelastic calculations and the prediction of flutter. Three-dimensional vortex flows have not been included in this survey as this is a fast evolving topic by itself. The subject has been differentiated with respect to the difficulty of flow modeling and computational requirements by distinguishing the status of the unsteady flows as: I, attached flow; II, mixed attached and separated flow; and III, separated flow.

1. For type I flows, computational methods have matured with a steady progression of improved techniques for flow simulation. Significant efforts have been devoted to understanding the effects of equation level, computational grid, boundary conditions, and viscous boundary layer modeling. Extensive comparisons with experimental data sets have been made with potential, Euler and Navier-Stokes equation solvers for two-dimensional airfoil cases and an understanding of the range of validity of the various methods can be made. Less extensive comparisons are available for three-dimensional wings and more evaluations are required before definite conclusions can be made.

2. Progress in solution algorithms for unsteady aerodynamics has been significant with large decreases in required computer resources due to the larger time steps allowed by more stable solution algorithms. Development of programs treating more realistic configurations such as multiple lifting surfaces and wing appendages are anticipated in the near future. The treatment of body conforming grids for deforming elastic vehicles must be addressed in order to fully utilize these emerging methods.
3. There is a need for experimental data sets with which to validate unsteady aerodynamic codes simulating these more complete configurations.
4. Many more transonic flutter calculations are needed before an assessment of the range of validity of the computational methods can be made. Of the few reported flutter calculations, a tendency is noted of predicting a premature upturn in the flutter boundary, very possibly due to violation of flow modeling assumptions (e.g. onset of type II unsteady flow).
5. Type II periodic aerodynamic oscillations about an 18 percent thick circular arc airfoil have been calculated with an upwind differenced Navier-Stokes code using flux splitting, duplicating earlier calculations by Levy. More insight into this case is provided by a transonic small disturbance potential code using nonisentropic modifications. Calculations of flap oscillations for this case illustrate the frequency dependence of the oscillations and gives further evidence of an aerodynamic resonance phenomena in the inviscid flow about airfoils at transonic speeds. Interaction of such type II flows with structural vibration characteristics may be expected to lead to "nonclassical" aeroelastic response.

References

[1]McCroskey, W. J.; Kutler, P.; and Bridgeman, J. O.: "Status and Prospects of Computational Fluid Dynamics for Unsteady Transonic Viscous Flows." In AGARD CP-374, "Transonic Unsteady Aerodynamics and its Aeroelastic Application," January 1985.

[2]Anon: "Military Specification; Airplane Strength and Rigidity; Flutter, Divergence, and Other Aeroelastic Instabilities." MIL-A-008870A (USAF), March 1971.

[3]Newsome, R. W.; and Kandil, O. A.: "Vortical Flow Aerodynamics - Physical Aspects and Numerical Simulation." AIAA Paper 87-0205, Reno, Nevada, January 1987.

[4]Tijdeman, H.: "Investigations of the Transonic Flow Around Oscillating Airfoils." National Aerospace Laboratory NLR, The Netherlands, NLR TR 77090U, 1978.

[5]Magnus, R.; and Yoshihara, H.: "The Transonic Oscillating Flap." AIAA Paper No. 76-327, presented at the AIAA 9th Fluid and Plasma Dynamics Conference, San Diego, California, July 14-16, 1976.

[6]Ballhaus, W. F.; and Goorjian, P. M.: "Implicit Finite-Difference Computations of Unsteady Transonic Flows about Airfoils." AIAA Journal, Vol. 15, No. 12, December 1977.

[7]Ballhaus, W. F.: "Some Recent Progress in Transonic Flow Computations." VKI Lecture Series: Computational Fluid Dynamics, von Karman Institute for Fluid Dynamics, Rhode-St-Genese, Belgium, March 1976.

[8]Bland, S. R.: "AGARD Two-Dimensional Aeroelastic Configurations." AGARD-AR-156, 1979.

[9]Bland, S. R.: "AGARD Three-Dimensional Aeroelastic Configurations." AGARD-AR-167, 1982.

[10]Lambourne, N. C.: "Compendium of Unsteady Aerodynamic Measurements." AGARD Report No. 702, 1982.

[11]Dau, K.; Vogel, S.; and Zimmerman H.: "Compendium of Unsteady Aerodynamic Measurements Addendum No. 1." AGARD Report No. 702, 1985.

[12]Mabey, D. G.; Welsh, B. L.; and Pyne, C. R.: "Measurements of Steady and Oscillatory Pressure on a Rectangular Wing." RAE TR 86040, July 1986.

[13]Sandford, M. C.; Ricketts, R. H.; and Hess, R. W.: "Recent Transonic Unsteady Pressure Measurements at the NASA Langley Research Center." Paper No. 85-23, presented at the Second International Symposium on Aeroelasticity and Structural Dynamics, Aachen, Germany, April 1-3, 1985.

[14]Tijdeman, H. et al.: "Transonic Wind Tunnel Tests on an Oscillating Wing with External Stores." AFFDL-TR-78-194, Pts. 1-IV, December 1978.

[15]Magnus, R. J.: "Calculations of Some Unsteady Transonic Flows about the NACA 64A006 and 64A010 Airfoils." Technical Report AFFDL-TR-77-46, July 1977.

[16]Magnus, R. J.: "Some Numerical Solutions of Inviscid, Unsteady, Transonic Flows Over the NLR 7301 Airfoil." CASD/LVP 78-013, Convair Division of General Dynamics, San Diego, California, January 1978.

[17]Steger, J. L.; and Bailey, H. E.: "Calculation of Transonic Aileron Buzz." AIAA Journal, Vol. 18, No. 3, March 1980.

[18]Chyu, W. J.; Davis, S. S.; and Chang, K. S.: "Calculation of Unsteady Transonic Flow Over an Airfoil." AIAA Journal, Vol. 19, No. 6, June 1981.

[19]Chyu, W. J.; and Davis, S. S.: "Numerical Studies of Unsteady Transonic Flow Over an Oscillating Airfoil." In AGARD CP-374, "Transonic Unsteady Aerodynamics and its Aeroelastic Application", January 1985.

[20]Borland, C. J.; Rizzetta, D. P.; and Yoshihara, H.: "Numerical Solution of Three-Dimensional Unsteady Transonic Flow Over Swept Wings." AIAA Journal, Vol. 20, No. 3, March 1982.

[21]Borland, C. J.; and Rizzetta, D. P.: "Nonlinear Transonic Flutter Analysis." AIAA Journal, Vol. 20, No. 11, November 1982.

[22]Laurent, A.: "Calcul D'Ecoulement Transsonique Instationnaire Authour D'Aile A Forte Fleche." In AGARD CP-374, "Transonic Unsteady Aerodynamics and its Aeroelastic Application," January 1985.

[23]Batina, J. T.: "An Efficient Algorithm for Solution of the Unsteady Transonic Small-Disturbance Equation." AIAA Paper No. 87-0109, Reno, Nevada, January 1987.

[24]Malone, J. B.; Sankar, L. N.; and Sotomayer, W. A.: "Unsteady Aerodynamic Modeling of a Fighter Wing in Transonic Flow." Journal of Aircraft, Vol. 23, No. 8, August 1986.

[25]Shankar, V.; and Ide, H.: "Treatment of Steady and Unsteady Flows Using a Fast, Time-Accurate Full Potential Scheme." AIAA Paper No. 85-4060, Colorado Springs, Colorado, October 1985.

[26]Isogai, K.: "The Development of Unsteady Transonic 3-D Full Potential Code and Its Aeroelastic Applications." In AGARD CP-374, "Transonic Unsteady Aerodynamics and its Aeroelastic Application," January 1985.

[27]Mulak, P.; and Angelini, J.: "Amelioration et Extension D'Une Methode De Calcul D'Ecoulements Transsoniques Tridimensionnels." In AGARD CP-374, "Transonic Unsteady Aerodynamics and its Aeroelastic Application," January 1985.

[28]Belk, D. M.; Janus, J. M.; and Whitfield, D. L.: "Three-Dimensional Unsteady Euler Equations Solutions on Dynamic Grids." AIAA Paper No. 85-1704, July 1985.

[29]Janus, J. M.: "The Development of a Three-Dimensional Split Flux Vector Euler Solver with Dynamic Grid Applications." M.S. Thesis, Mississippi State, Mississippi, August 1984.

[30]Sides, J.: "Computation of Unsteady Transonic Flows with an Implicit Numerical Method for Solving the Euler Equations." Rech. Aerosp. 1985-2.

[31]Jameson, A.; and Venkatakrishnan, V.: "Transonic Flows About Oscillating Airfoils Using the Euler Equations." AIAA Paper No. 85-1514, AIAA 7th Computational Fluid Dynamics Conference, 1985.

[32]Smith, G. E.; Whitlow, W., Jr.; and Hassan, H. A.: "Unsteady Transonic Flows Past Airfoils Using the Euler Equations." AIAA Paper No. 86-1764-CP, San Diego, California, June 9-11, 1986.

[33]Salmond, D. J.: "Calculation of Harmonic Aerodynamic Forces on Aerofoils and Wings from the Euler Equations." In AGARD CP-374, "Transonic Unsteady Aerodynamics and its Aeroelastic Application," January 1985.

[34]Belk, Dave M.: "Unsteady Three-Dimensional Euler Equations Solutions on Dynamic Blocked Grids." Ph.D dissertation, Mississippi State University, August 1986.

[35]McDevitt, J. B.; Levy, L. L., Jr.; and Deiwert, G. S.: "Transonic Flows about a Thick Circular-Arc Airfoil." AIAA Journal, Vol. 14, No. 5, May 1976.

[36]McDevitt, J. B.: "Supercritical Flow About a Thick Circular-Arc Airfoil." NASA TM 78549, January 1979.

[37]Levy, L. L., Jr.: "Experimental and Computational Steady and Unsteady Transonic Flows about a Thick Airfoil." AIAA Journal, Vol. 16, No. 6, June 1978.

[38]Mabey, D. G.: "Oscillatory Flows from Shock-Induced Separations on Biconvex Aerofoils of Varying Thickness in Ventilated Wind Tunnels." AGARD CP 296, 1980.

[39]Mabey, D. G.; Welsh, B. L.; and Cripps, B. E.: "Periodic Flows on a Rigid 14% Thick Biconvex Wing at Transonic Speeds." RAE Technical Report 81059, May 1981.

[40]Levy, L. L., Jr.: "Predicted and Experimental Steady and Unsteady Transonic Flows About a Biconvex Airfoil." NASA TM 81262, February 1981.

[41]Mabey, D. G.; Ashill, P. R.; and Welsh, B. L.: "Aeroelastic Oscillations Caused by Transitional Boundary Layers and Their Attenuation." AIAA Paper No. 86-0736, West Palm Beach, Florida, March 1986.

[42]Osswald, G. A.; Ghia, K. N.; and Ghia, U.: "An Implicit Time-Marching Method for Studying Unsteady Flow with Massive Separation." AIAA Paper No. 85-1489, AIAA 7th Computational Fluid Dynamics Conference, 1985.

[43]Lecointe, Y.; and Piquet, J.: "Unsteady Viscous Flow Round Moving Circular Cylinders and Airfoils." AIAA Paper No. 85-1490, AIAA 7th Computational Fluid Dynamics Conference, 1985.

[44]Anderson, W. K.; Thomas, J. L.; and Rumsey, C. L.: "Application of Thin Layer Navier-Stokes Equations Near Maximum Lift." AIAA Paper No. 84-0049, presented at the AIAA 22nd Aerospace Sciences Meeting, Reno, Nevada, January 1984.

[45]Anon: "Unsteady Aerodynamics." AGARD-CP-227, 1978.

[46]Anon: "Boundary Layer Effects on Unsteady Airloads." AGARD-CP-296, 1981.

[47]"Transonic Unsteady Aerodynamics and its Aeroelastic Applications." AGARD-CP-374, 1985.

[48]Anon: "Unsteady Aerodynamics-Fundamentals and Applications to Aircraft Dynamics." AGARD-CP-386, 1985.

[49]Peterson, V. L.: "Trends in Computational Capabilities for Fluid Dynamics." In AGARD CP-375, "Transonic Unsteady Aerodynamics and its Aeroelastic Application," January 1985.

[50]Mykytow, W. J.: "Transonic Unsteady Aerodynamics and its Aeroelastic Applications." In AGARD CP-386, Unsteady Aerodynamics - Fundamentals and Applications to Aircraft Dynamics," November 1985.

[51]Mabey, D. G.; and Chambers, J. R.: "Unsteady Aerodynamics - Fundamentals and Applications to Aircraft Dynamics." AGARD-AR-222, May 1985.

[52]Zwaan, R. J.: "Aeroelastic Problems of Wings in Transonic Flow." Presented at VKI Lecture Series "Unsteady Airloads and Aeroelastic Problems in Separated and Transonic Flow," Rhode-Saint-Genese, Belgium, March 1981. (Also NLR MP 81005 U).

[53]Deiwert, G. S.: "Finite Difference Simulation of Unsteady Interactive Flows." In Computational Methods in Viscous Flow, ed. by Habashi, W. G.; Pineridge Press, 1984.

[54]Mabey, D. G.: "A Review of Some Recent Research on Time-Dependent Aerodynamics." The Aeronautical Journal of The Royal Aeronautical Society, February 1984.

[55]Pearcy, H. H.; Haines, A. B.; and Osborne, J.: "The Interaction Between Local Effects at the Shock and Real Separation." In AGARD CP No. 35, Transonic Aerodynamics, 1968.

[56]Bradley, R. G.: "Practical Aerodynamic Problems - Military Aircraft." In Transonic Aerodynamics, ed by Nixon, D., Vol. 81, Progress in Astronautics and Aeronautics, AIAA, 1982.

[57]Farmer, M. G.; Hanson, P. W.; and Wynne, E. C.: "Comparison of Supercritical and Conventional Wing Flutter Characteristics." NASA TM X-72837, May 1976.

[58]Erickson, L. L.: "Transonic Single-Mode Flutter and Buffet of a Low Aspect Ratio Wing Having a Subsonic Airfoil Shape." NASA TN D-7346, January 1974.

[59]Houwink, R.; Kraan, A. N.; and Zwaan, R. J.: "A Wind-Tunnel Study of the Flutter Characteristics of a Supercritical Wing." Paper No. 81-0651. Journal of Aircraft, Vol. 19, May 1982, pp. 400-405.

[60]Persoon, A. J.; Horsten, J. J.; and Meijer, J. J.: "On Measuring Transonic Dips in the Flutter Boundaries of a Supercritical Wing in the Wind Tunnel." AIAA Paper No. 83-1031-CP, May 1983. Also NLR MP 83008 U, January 1983.

[61]Moss, G. F.; and Pierce, D.: "The Dynamic Response of Wings in Torsion at High Subsonic Speeds." In AGARD CP-226, 1977.

[62]Davis, S. D.; and Malcolm, G. N.: "Transonic Shock-Wave/Boundary-Layer Interactions on an Oscillating Airfoil." AIAA Journal, Vol. 18, No. 11, November 1980.

[63]McDevitt, J. B.; and Okuno, A. F.: "Static and Dynamic Pressure Measurements on a NACA 0012 Airfoil in the Ames High Reynolds Number Facility." NASA Technical Paper 2485, June 1985.

[64]Zimmerman, H.: "The Application of Transonic Unsteady Methods for Calculation of Flutter Airloads." In AGARD CP-374 "Transonic Unsteady Aerodynamics and its Aeroelastic Application," January 1985.

[65]den Boer, R. G.; and Houwink, R.: "Analysis of Transonic Aerodynamic Characteristics for a Supercritical Airfoil Oscillating in Heave, Pitch and With Oscillating Flap." In AGARD CP-374, "Transonic Unsteady Aerodynamics and its Aeroelastic Application," January 1985.

[66]Le Balleur, J. C.; and Girodroux-Lavigne, P.: "Prediction of Buffeting and Calculation of Unsteady Boundary Layer Separation Over Airfoils." Presented at IUTAM Symposium on "Boundary Layer Separation, London, University College, August 1986.

[67]Hess, R. W.; Seidel, D. A.; Igoe, W. B.; and Lawing, P. L.: "Highlights of Unsteady Pressure Tests on a 14 Percent Supercritical Airfoil at High Reynolds Number, Transonic Condition." AIAA Paper No. 87-0035, Reno, Nevada, January 12-15, 1987.

[68]Sandford, M. C.; Ricketts, R. H.; and Hess, R. W.: "Recent Transonic Unsteady Presure Measurements at the NASA Langley Research Center." Paper No. 85-23, Second International Symposium On Aeroelasticity and Structural Dynamics, Aachen, Germany, April 1-3, 1985.

[69]Ricketts, R. H.; Sandford, M. C.; Watson, J. J.; and Seidel, D. A.: "Subsonic and Transonic Unsteady- and Steady-Pressure Measurements on a Rectangular Supercritical Wing Oscillated in Pitch." NASA TM 85765, August 1984.

[70]Mabey, D. G.; Welsh, B. L.; and Cripps, B. E.: "Measurements of Steady and Oscillatory Pressures on a Low Aspect Ratio Model at Supersonic and Supersonic Speeds," RAE TR 84095, September 1984.

[71]Isogai, K.; and Suetsugu, K.: "Numerical Simulation of Transonic Flutter of a Supercritical Wing." NAL Report TR-726T, August 1982.

[72]Bennett, R. M.; Seidel, D. A.; and Sandford, M. C.: "Transonic Calculations for a Flexible Supercritical Wing and Comparison with Experiment." AIAA Paper No. 85-0665-CP, Orlando, Florida, April 15-17, 1985.

[73]Seidel, D. A.; Sandford, M. C.; and Eckstrom, C. V.: "Measured Unsteady Transonic Aerodeynamic Characteristics of an Elastic Supercritical Wing with an Oscillating Control Surface." AIAA Paper No. 85-0598-CP, Orlando, Florida, April 15-17, 1985.

[74]Guruswamy, P.; and Goorjian, P. M.; and Tu, E. L.: "Transonic Aeroelasticity of Wings With Tip Stores." AIAA Paper No. 86-1007-CP, San Antonio, Texas, May 19-21, 1986.

[75]Deiwert, G. S.: "Computation of Separated Transonic Turbulent Flows." AIAA Paper No. 75-829, Hartford, Connecticut, June 1975.

[76]Seidel, D. A.; Bennett, R. M.; and Ricketts, R. H.: "Some Recent Applications of XTRAN3S." AIAA Paper No. 83-1811, Danvers, Mass., July 1983.

[77]Ruo, S. Y.; Malone, J. B.; and Sankar, L. N.: "Steady and Unsteady Full Potential Calculations for High and Low Aspect Ratio Supercritical Wings." AIAA Paper No. 86-0122, Reno, Nevada, January 6-9, 1986.

[78]Rizzetta, D. P.; and Chin, W. C.: "Effect of Frequency in Unsteady Transonic Flows." AIAA Journal, Vol. 12, No. 7, July 1979.

[79]Houwink, R.; and van der Vooren, J.: "Improved Version of LTRAN2 for Unsteady Transonic Flow Computations." AIAA Journal, Vol. 18, August 1980.

[80]Isogai, K.: "Numerical Study of Transonic Flutter of a Two-Dimensional Airfoil." NAL Report TR-716T, July 1980.

[81]Hessenius, K. A.; and Goorjian, P. M.: "Validation of LTRAN2-HI By Comparison with Unsteady Transonic Experiment." AIAA Journal, Vol. 20, No. 5, May 1982.

[82]Chow, L. J.; and Goorjian, P. M.: "Implicit Unsteady Transonic Airfoil Calculations at Supersonic Freestreams." AIAA Paper No. 82-0934, St. Louis, Missouri, June 7-11, 1982.

[83]Bland, S. R.; and Edwards, J. W.: "Airfoil Shape and Thickness Effects on Transonic Airloads and Flutter." Journal of Aircraft, Vol. 21, No. 3, March 1984.

[84]Goorjian, P. M.; Meagher, M. E.; and Buskirk, R. V.: "Monotone Switches in Implicit Algorithms for Potential Equations Applied to Transonic Flows." AIAA Journal, Vol. 23, No. 4, April 1985.

[85]Engquist, B. E.; and Osher, S. J.: "Stable and Entropy Satisfying Approximations for Transoic Flow Calculations." Journal of Computation, Vol. 34, No. 149, January 1980.

[86]Kwak, D.: "Nonreflecting Far-Field Boundary Conditions for Unsteady Transonic Flow." AIAA Journal, Vol. 19, No. 11, November 1981.

[87]Whitlow, Woodrow, Jr.: "XTRAN2L: A Program for Solving the General-Frequency Unsteady Transonic Small Disturbance Equation." NASA TM 85723, November 1983.

[88]Houwink, R.: "Unsteady Viscous Transonic Flow Computations Using the LTRAN2-NLR Code Coupled with Green's Lag-Entrainment Method." In Numerical and Physical Aspects of Aerodynamic FlowsII, Chapter 15, ed. T. Cebici, Springer, New York, 1984.

[89]Edwards, J. W.; Bland, S. R.; and Seidel, D. A.: "Experience with Transonic Unsteady Aerodynamic Calculations." In AGARD CP-374, "Transonic Unsteady Aerodynamics and its Aeroelastic Application, January 1985.

[90]Bland, S. R.; and Seidel, D. A.: "Calculation of Unsteady Aerodynamics for Four AGARD Standard Aeroelastic Configurations." NASA TM 85817, May 1984.

[91]Goorjian, P. M.; and Guruswamy, G. P.: "Unsteady Transonic Aerodynamic and Aeroelastic Calculations About Airfoils and Wings." In AGARD CP-374, "Transonic Unsteady Aerodynamics and its Aeroelastic Application,"January 1985.

[92]Malone, J. B.; Ruo, S. Y.; and Sankar, N. L.: "Computation of Unsteady Transonic Flows About Two-Dimensional and Three-Dimensional AGARD Standard Configurations." In AGARD CP-374, "Transonic Unsteady Aerodynamics and its Aeroelastic Application," January 1985.

[93]Edwards, J. W.: "Applications of Potential Theory Computations to Transonic Aeroelasticity." Paper No. ICAS-86-2.9.1, Fifteenth Congress of the International Council fo the Aeronautical Sciences, London, England, September 1986.

[94]Batina, J. T.: "Effects of Airfoil Shape, Thickness, Camber, and Angle of Attack on Calculated Transonic Unsteady Airloads." NASA TM 86320, March 1985.

[95]Berry, H. M.; Batina, J. T.; and Yang, T. Y.: "Viscous Effects on Transonic Airfoil Stability and Response." Journal of Aircraft, Vol. 23, No. 5, May 1986, pp. 361-369.

[96]Steinhoff, J.; and Jameson, A.: "Multiple Solutions of the Transonic Potential Flow Equation." AIAA Journal, Vol. 20, No. 11, November 1982.

[97]Williams, M. H.; Bland, S. R.; and Edwards, J. W.: "Flow Instabilities in Transonic Small-Disturbance Theory." AIAA Journal, Vol. 23, No. 10, October 1985.

[98]Fuglsang, D. F.; and Williams, M. H.: "Non-Isentropic Unsteady Transonic Small Disturbance Theory." AIAA Paper No. 85-0600, Orlando, Florida, April 1985.

[99]Gibbons, M. D.; Whitlow, W., Jr.; and Williams, M. H.: "Nonisentropic Unsteady Three Dimensional Small Disturbance Potential Theory." AIAA Paper 86-0863, San Antonio, TX, May 1986.

[100]Osher, S.; Hafez, M.; and Whitlow, Woodrow, Jr.: "Entropy Condition Satisfying Approximations for the Full Potential Equation of Transonic Flow." Mathematics of Computations, Vol. 44, No. 169, January 1985.

[101]Whitlow, W., Jr.; Hafez, M. H.; and Osher, S. J.: "An Entropy Correction Method for Unsteady Full Potential Flows with Strong Shocks." AIAA Paper No. 86-1768-CP, San Diego, California, June 9-11, 1986.

[102]Steger, J. L.: "Implicit Finite-Difference Simulation of Flow about Arbitrary Two-Dimensional Geometries." AIAA Journal, Vol. 16, No. 7, July 1978.

[103]Sankar, L. M.; Ruo, S. Y.; and Malone, J. B.: "Application of Surface Transpiration in Computational Aerodynamics." AIAA Paper No. 86-0511, Reno, Nevada, January 6-9, 1986.

[104]Couston, M.; Angelini, J. J., Le Balleur, J. C.; and Girodroux-Lavigne, P.: Prise En Compte Deffets De Couche Limite Instationnaire Dans Un Calcul Bidimensionnel Transsonique." In AGARD CP-296, "Boundary Layer Effects on Unsteady Airloads," 1981.

[105]Couston, M.; Angelini, J. J.; et Mulak, P.: "Application de L'equation des petites perturbations transonniques aux calculs d'ecoulements bidimensionnels instationnaires." Rech. Aerosp., No. 1975-5, 1975, pp. 325-340.

[106]Le Balleur, J. C.: "Numerical Viscid-Inviscid Interaction in Steady and Unsteady Flows." Proc. 2nd Symposium on Numerical and Physical Aspects of Aerodynamic Flows, California State University, Long Beach, California, 1983.

[107]Le Balleur, J. C.; and Girodroux-Lavigne, P.: "A Semi-Implicit and Unsteady Numerical Method of Viscous-Inviscid Interaction for Transonic Separated Flows." Rech. Aerosp. 1984-1, 1984, pp. 14-37.

[108]Girodroux-Lavigne, P.; and Le Balleur, J. C.: "Calcul D'Ecoulements Instationnaires Transsoniques Avec Decollements Par Interaction Visqueux - Non Visqueux." In AGARD CP-374, "Transonic Unsteady Aerodynamics and its Aeroelastic Application," January 1985.

[109]Le Balleur, J. C.; and Girodroux-Lavigne, P.: "A Viscous-Inviscid Interaction Method for Computing Unsteady Transonic Separation." Proc. 3rd Symposium on Numerical and Physical Aspects of Aerodynamic Flows, ed. T. Cebici, Springer-Verlag, 1986.

[110]Houwink, R.: "Computations of Separated Subsonic and Transonic Flow About Airfoils in Unsteady Motion." NLR MP 84-0944, Amsterdam, 1984.

[111]Rizzetta, D. P.: "Procedures for the Computation of Unsteady Transonic Flows Including Viscous Effects." NASA CR 166249, January 1982.

[112]Rizzetta, D. P.; and Borland, C. J.: "Unsteady Transonic Flow Over Wings Including Inviscid/Viscous Interaction." Journal of Aircraft, Vol. 21, No. 3, March 1983.

[113]Guruswamy, P.; and Goorjian, P. M.: "Effects of Viscosity on Transonic-Aerodynamic and Aeroelastic Characteristics of Oscillating Airfoils." Journal of Aircraft, Vol. 21, No. 9, September 1984.

[114]Marstiller, J. W.; Guruswamy, P.; Yang, T. Y.; and Goorjian, P. M.: "Effects of Viscosity and Modes on Transonic Flutter Boundaries of Wings." AIAA Paper No. 84-0870, Palm Springs, CA, 1984.

[115]Howlett, J. T.: "Efficient Self-Consistent Viscous-Inviscid Solutions for Unsteady Transonic Flow." AIAA Paper No. 85-0482, Reno, Nevada, January 1985.

[116]Guruswamy, G. P.; and Goorjian, P. M.: "Efficient Algorithm for Unsteady Transonic Aerodynamics of Low-Aspect-Ratio Wings." Journal of Aircraft, Vol. 22, No. 3, March 1985.

[117]Malone, J. B.; and Sankar, N. L.: "Numerical Simulation of Two Dimensional Unsteady Transonic Flows Using the Full-Potential Equation." Journal of Aircraft, Vol. 22, No. 8, August 1984.

[118]Malone, J. B.; and Sankar, N. L.: "Numerical Solutions of 2-D Unsteady Transonic Flows Using Coupled Potential-Flow/Boundary-Layer Methods." AIAA Paper No. 84-0268, Reno, Nevada, January 9-12, 1984.

[119]Hafez, M. M.; Osher, S.; and Whitlow, W., Jr.: "Improved Finite Difference Schemes for Transonic Potential Calculations." AIAA Paper No. 84-0092, Los Angeles, California, January 1984.

[120]Shankar, V.; Ide, H.; Gorski, J.; and Osher, S.: "A Fast, Time Accurate Unsteady Full Potential Scheme." AIAA Paper No. 85-1512-CP, Cincinnati, Ohio, 1985.

[121]Steger, J. L.; and Warming, R. F.: "Flux Vector Splitting of the Inviscid Gasdynamic Equations with Application to Finite-Difference Methods." Journal of Computational Physics, Vol. 40, 1981, pp. 263-293.

[122]Harten, A.; Lax, P. D.; and Van Leer, B.: "On Upstream Differencing and Godunov-Type Schemes for Hyperbolic Conservation Laws." SIAM Review, Vol. 25, 1983, pp. 35-61.

[123]Chakravarthy, S.; and Osher, S.: "A New Class of High Accuracy TVD Schemes for Hyperbolic Conservation Laws." AIAA Paper 85-0363, January 1985.

[124]Thomas, J. L.; Van Leer, B.; and Walters, R. W.: "Implicit Split-Flux Schemes for the Euler Equations." AIAA 85-1680, July 1985.

[125]Yee, H. C.; and Harten, A.: "Implicit TVD Schemes for Hyperbolic Conservation Laws in Curvilinear Coordinates." AIAA Paper 85-1513(CP), July 1985.

[126]Chakravarthy, S. R.: "Relaxation Methods for Unfactored Implicit Schemes." AIAA Paper 84-0165, January 1984.

[127]Roe, P. L.: "Characteristics Based Schemes for the Euler Equations." Annual Review of Fluid Mechanics, Vol. 18, pp. 337-65, 1986.

[128]Coakley, T. J.: "Implicit Upwind Methods for the Compressible Navier-Stokes Equations." AIAA Paper 83-1958, July 1983.

[129]Thomas, J. L.; and Walters, R. W.: "Upwind Relaxation Algorithms for the Navier-Stokes Equations." AIAA Paper 85-1501, July 1985.

[130]Ying, S. X.; Steger, J. L.; Schiff, L. B.; and Baganoff, D.: "Numerical Simulation of Unsteady, Viscous, High-Angle-of-Attack Flows Using a Partially Flux-Split Algorithm." AIAA Paper 86-2179, August 1986.

[131]Anderson, W. K.; Thomas, J. L.; and Whitfield, D. C.: "Multigrid Acceleration of the Flux-Split Euler Equations." AIAA Paper 86-0274, January 1986.

[132]Anderson, W. K.: "Implicit Multigrid Algorithms for the Three-Dimensional Flux-Split Euler Equations." Ph.D. Dissertation, Mississippi State University, Mississippi, August 1986.

[133]Jesperson, D. C.: "A Time-Accurate Multiple-Grid Algorithm." AIAA Paper 85-1493(CP), July 1985.

[134]Batina, J. T.: "Unsteady Transonic Flow Calculations for Interfering Lifting Surface Configurations." NASA TM 86432, May 1985.

[135]Batina, J. T.: "Unsteady Transonic Flow Calculations for Wing- Fuselage Configurations." AIAA Paper No. 86-0862, San Antonio, Texas, May 1986.

[136]Shankar, V.; and Goebel, T.: "Computation of Canard-Wing Transonic Flows Using the Full Potential Equation." AIAA Paper No. 86-1795, San Diego,California, June 1986.

[137]Malone, J. B.; and Sankar, L. N.: "Unsteady Full Potential Calculations for Complex Wing-Body Configurations." AIAA Paper No. 85-4062, Colorado Springs, Colorado, October 14-16, 1985.

[138]Guruswamy, G. P.; Goorjian, P. M.; and Tu, E. L.: "Unsteady Transonics of a Wing with Tip Store." Journal of Aircraft, Vol. 23, No. 8, August 1986.

[139]Edwards, J. W.; Bennett, R. M.; Whitlow, W., Jr.; and Seidel, D. A.: "Time-Marching Transonic Flutter Solutions Including Angle-of-Attack Effects." AIAA Journal, Vol. 20, No. 11, November 1983.

[140]Guruswamy, P.; and Goorjian, P. M.: "Computations and Aeroelastic Applications of Unsteady Transonic Aerodynamics About Wings." Journal of Aircraft, Vol. 21, No. 1, January 1974, pp. 37-43.

[141]Myers, M. R.; Guruswamy, P.; and Goorjian, P. M.: "Flutter Analysis of a Transport Wing Using XTRAN3S." AIAA Paper No. 83-0922, 1983.

[142]Johnson, D. A.: "Predictions of Transonic Separated Flow with an Eddy-Viscosity/Reynolds-Shear Stress Closure Model." AIAA Paper No. 85-1683, July 1985.

[143]Simpson, R.: "A Review of Two-Dimensional Turbulent Separated Flow Calculation Methods." IUTAM Symposium on Boundary Layer Separation, August 1986.

[144]Coakley, T. J.: "Impact of Turbulence Modeling on Numerical Accuracy and Efficiency of Compressible Flow Simulations." 10th International Conference on Numerical Methods in Fluid Mechanics, Bejing, China, June 1986.

[145]Coakley, T. J.: "Numerical Method for Gas Dynamics Combining Characteristic and Conservation Concepts." AIAA Paper No. 81-1257, June 1981.

[146]Baldwin, B.; and Lomax, H.: "Thin-Layer Approximation and Algebraic Model for Separated Turbulent Flows." AIAA Paper No. 78-257, January 1978.

[147]Coakley, T. J.: "A Compressible Navier-Stokes Code for Turbulent-Flow Modeling." Workshop on Computational Fluid Dynamics held at the University of Tennessee Space Institute, March 12-16, 1984.

[148]Buning, P. G.; and Steger, J. L.: "Solution of the Two-Dimensional Euler Equations with Generalized Coordinate Transformation Using Flux Vector Splitting." AIAA Paper No. 82-0971, June 1982.

[149]Rumsey, C. L.; Thomas, J. L.; Warren, G. P.; and Liu, G. C.: "Upwind Navier-Stokes Solutions for Separated Periodic Flows." AIAA Paper No. 86-0247, presented at the AIAA 24th Aerospace Sciences Meeting, Reno, Nevada, January 1986.

[150]Thomas, J. L.; Walters, R. W.; Van Leer, B.; and Anderson, W. K.: "Implicit Finite-Volume Algorithms for the Flux-Split Euler Equations." Proceedings, GAMM Workshop on the Numerical Simulation of Compressible Euler Flows, Vieweg, in press.

[151]Barton, J. T.; and Pulliam, T. H.: "Airfoil Computation at High Angles of Attack, Inviscid and Viscous Phenomena." AIAA Journal, Vol. 24, No. 5, May 1986.

[152]Shamroth, S. J.: "Calculation of Steady and Oscillating Airfoil Flow Fields Via the Navier Stokes Equations." AIAA Paper No. 84-525, Reno, Nevada, January 1984.

[153]Sankar, L. N.; Malone, J. B.; and Schuster, D.: "Full Potential and Euler Solutions for the Unsteady Transonic Flow Past a Fighter Wing." AIAA Paper No. 85-4061, Colorado Springs, Colorado, October 1985.

[154]Houwink, R.; and Veldman, A. E. P.: "Steady and Unsteady Separated Flow Computations for Transonic Airfoils." AIAA Paper No. 84-1618, Snowmass, Colorado, June 1984.

[155]Bennett, R. M.; Wynne, E. C.; and Mabey, D. G.: "Calculation of Transonic Steady and Oscillatory Pressures on a Low Aspect Ratio Model and Comparison with Experiment." NASA TM 86449, June 1985.

[156]Ruo, S. Y.; and Malone, J. B.: "Steady and Unsteady Transonic Airloads on a Supercritical Wing." Journal of Aircraft, Vol. 22, No. 1, January 1985.

[157]Borland, C. J.; and Sotomayer, W. A.: "An Algorithm for Unsteady Transonic Flow About Tapered Wings." AIAA Paper No. 84-1567, Snowmass, Colorado, June 1984.

Table 2. References giving comparisons of experimental and calculated three-dimensional unsteady aerodynamics and aeroelasticity

	TSD	FP	EE
F-5 Model	115, 157, 137, 23	24, 136, 153, 102	
NORA	76, 22	64, 26	
LANN	100, 156	45, 40, 24, 76	
RAE Wing A		64, 43, 26, 136	
RSW	116, 75	40, 66, 76, 25	96, 34
RAE Tailplane	114, 85+, 155, 98+		75, 33
Other	118*, 113*, 71*, 73*	64*, 65*, 26*, 70*	

+ Nonisentropic corrections
• Aeroelastic and flutter comparisons

Table 1 References giving comparisons of experimental and calculated two-dimensional unsteady aerodynamics

	TSD	FP	EE	NS
NACA 64A006	6, 103*, 88, 89, 87*	102, 116	5, 15	
NACA 64A010A	80, 82, 138, 88, 89, 112*, 87*, 93, 97+, 114*, 105*-108*	117, 116, 79, 119	15, 30, 32	19, 18
NACA 0012	88, 90*, 109*, 97+, 96+, 93	119, 100+	29, 28, 31	152, 44, 148 43, 154
NLR 7301	89, 88, 107*, 114*, 97+	117	16, 30, 32	
MBB A-3	112*, 89, 82, 138, 114*, 63			
Supercritical Airfoils	154*, 109*, 65*, 66			
Circular arc Airfoils	106*, 107*, 108*			35, 37, 36, 40
Other			151	17, 42, 43, 148

• Interacted boundary layer model
+ Nonisentropic corrections

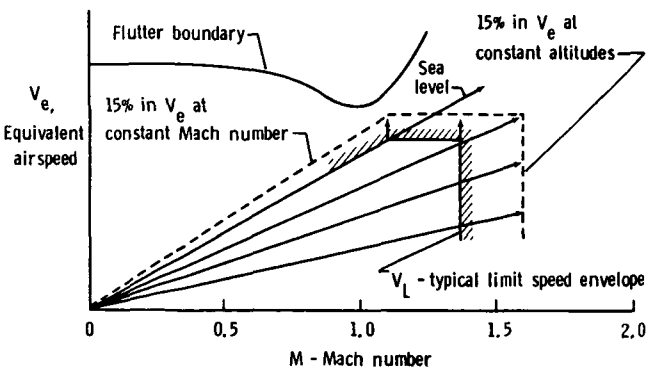

Fig. 1 Graphical representation of minimum required flutter margin, (Ref. 2).

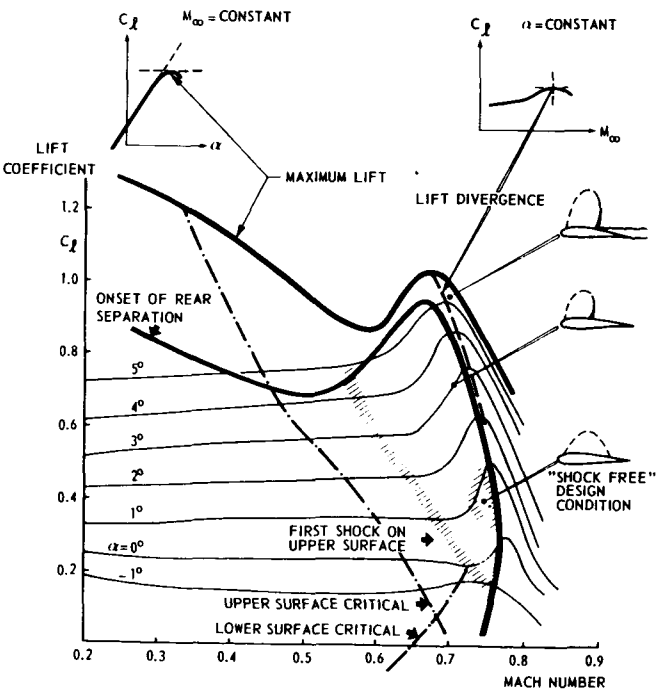

Fig. 2 Main characteristics and boundaries for the onset of separation for the NLR 7301 supercritical airfoil. (Tijdeman, Ref. 4)

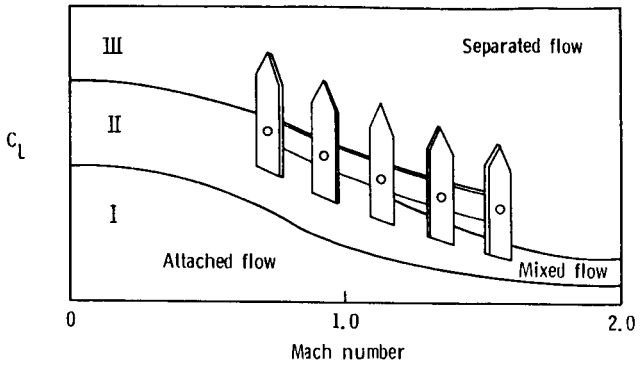

Fig. 3 Characteristics of attached and separated flow for complete aircraft. (after Bradley, Ref. 56)

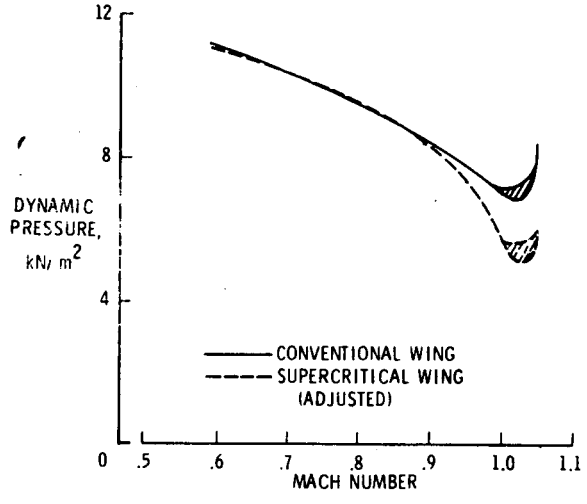

Fig. 4 Comparison of conventional wing flutter boundary with adjusted supercritical wing boundary. (Farmer et al., Ref. 57)

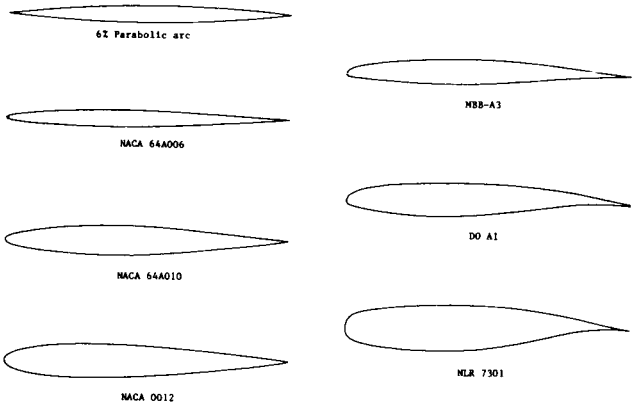

Fig. 5 AGARD Structures and Materials Panel two-dimensioal standard aeroelastic configurations. (Bland, Ref. 8)

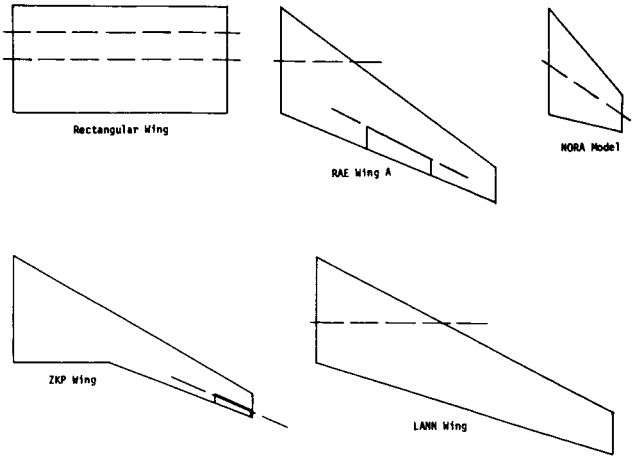

Fig. 6 AGARD Structures and Materials Panel three-dimensional standard aeroelastic configurations. (Bland, Ref. 9)

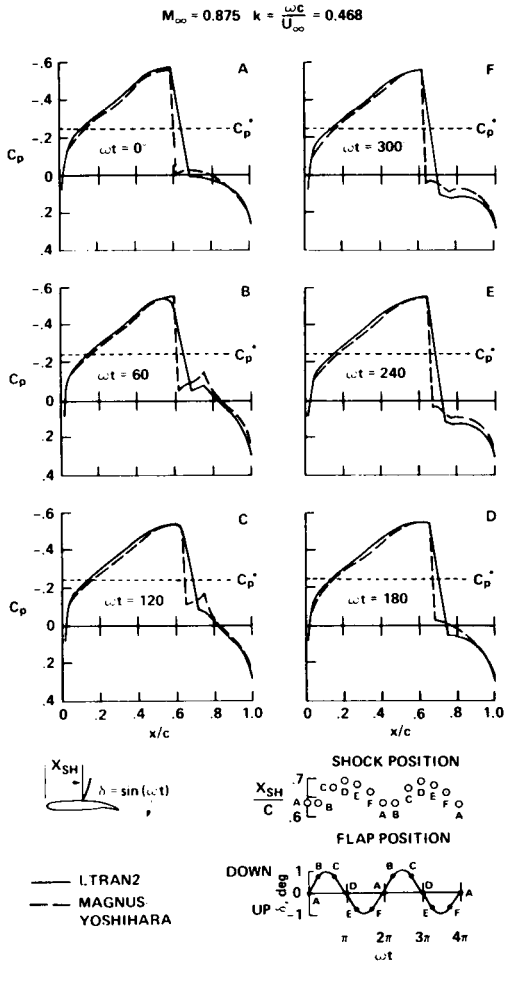

(a) Type A shock motion.

Fig. 7 Upper surface pressure coefficients of an NACA 64A006 airfoil with oscillating trailing-edge flap showing type A, B, and C shock motions. (Ballhaus and Goorjian, Ref. 6)

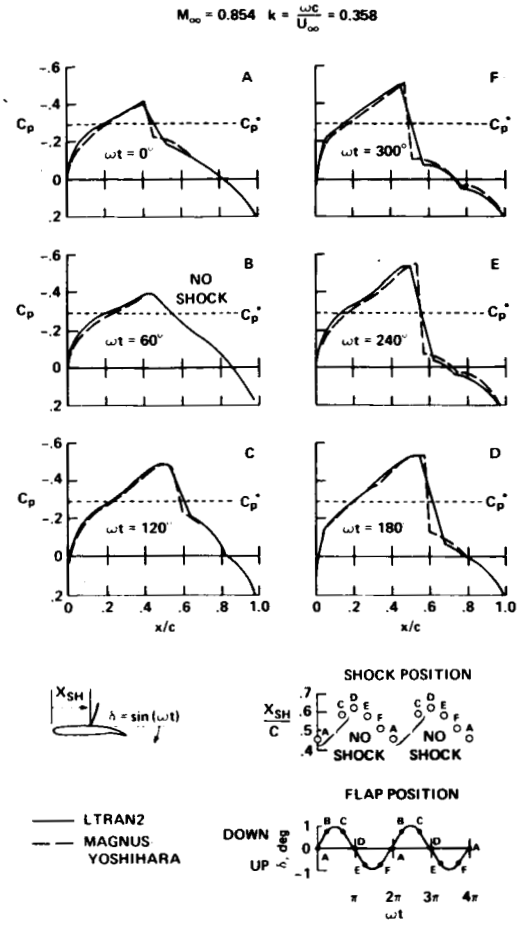

(b) Type B shock motion.

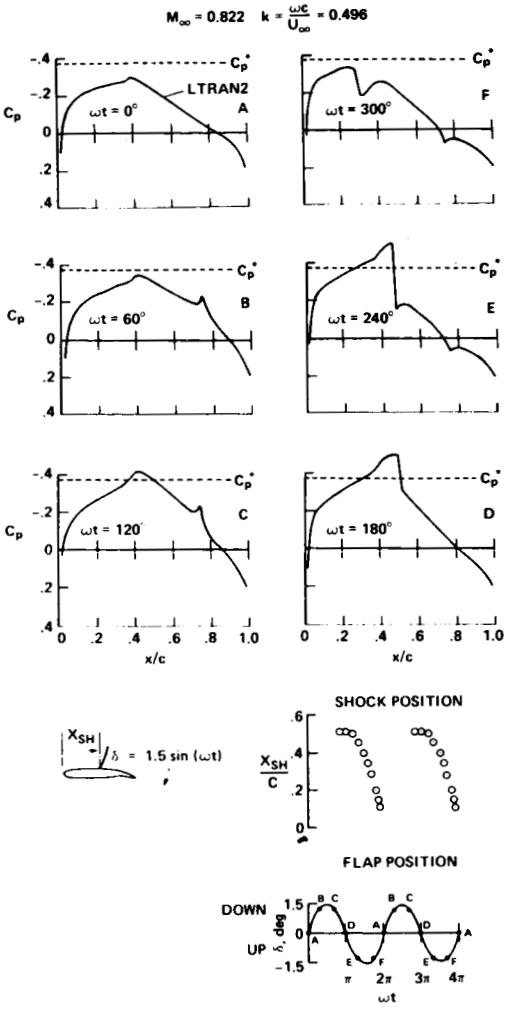

(c) Type C shock motion.

Fig. 7 Continued.

Fig. 7 Concluded.

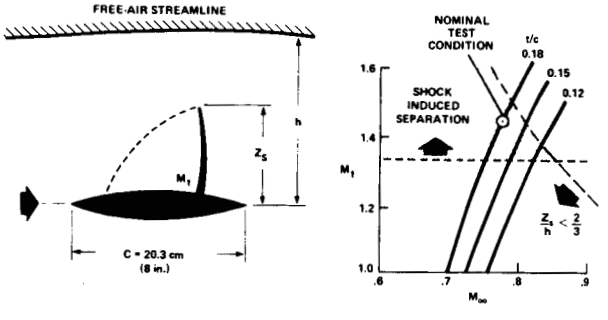

Fig. 8 Eighteen percent thick circular arc airfoil experimental conditions. (McDevitt, Ref. 36)

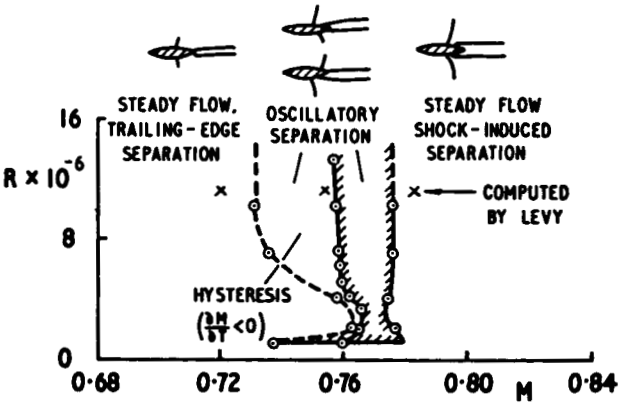

Fig. 9 Steady and oscillatory flow domains for an 18 percent thick circular arc airfoil. (Levy, Ref. 37)

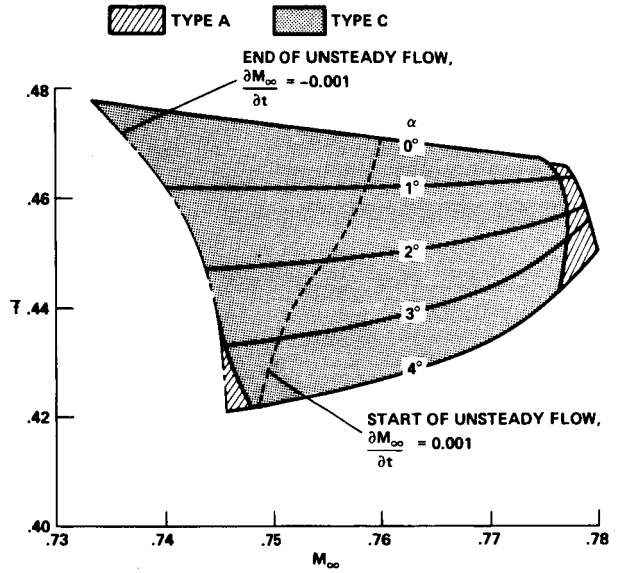

Fig. 10 Reduced frequency of periodic oscillations on an 18 percent thick circular arc airfoil for varying angle of attack.
(McDevitt, Ref. 36)

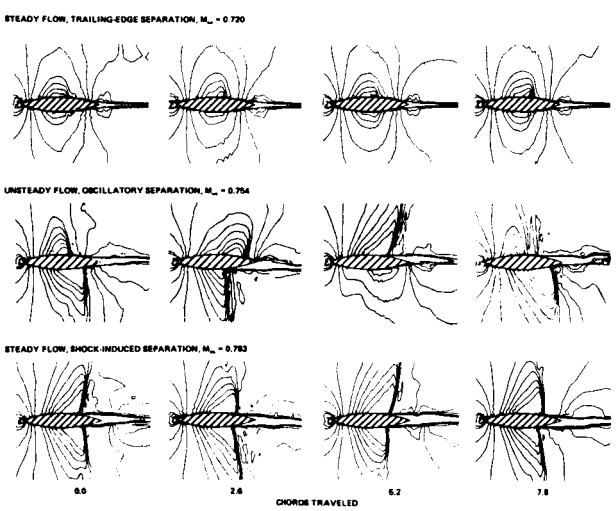

Fig. 11 Computed Mach contours for 18 percent circular arc airfoil, M = 0.72, 0.75, and 0.78, $Re_c = 11 \times 10^6$.
(Levy, Ref. 37)

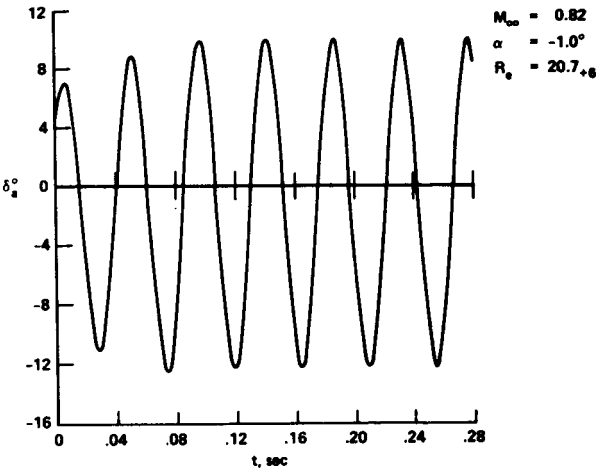

Fig. 12 Computed variation of aileron angle with time showing buzz conditon.
(Steger and Bailey, Ref. 17)

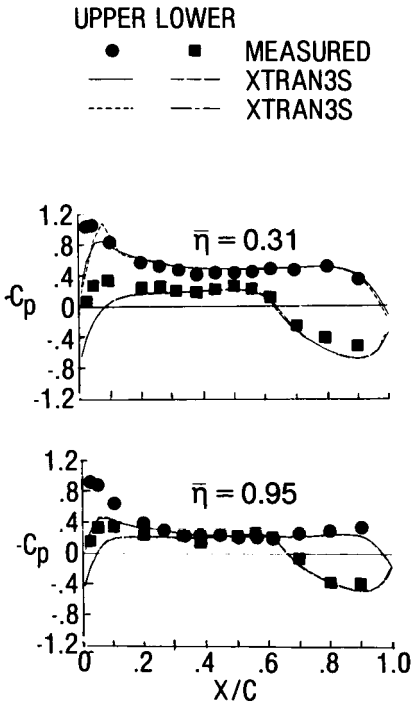

(a) Steady pressures

Fig. 13 Comparison of measured and calculated steady and unsteady pressures for the NASA rectangular supercritical wing.
(Seidel et al., Ref. 76)

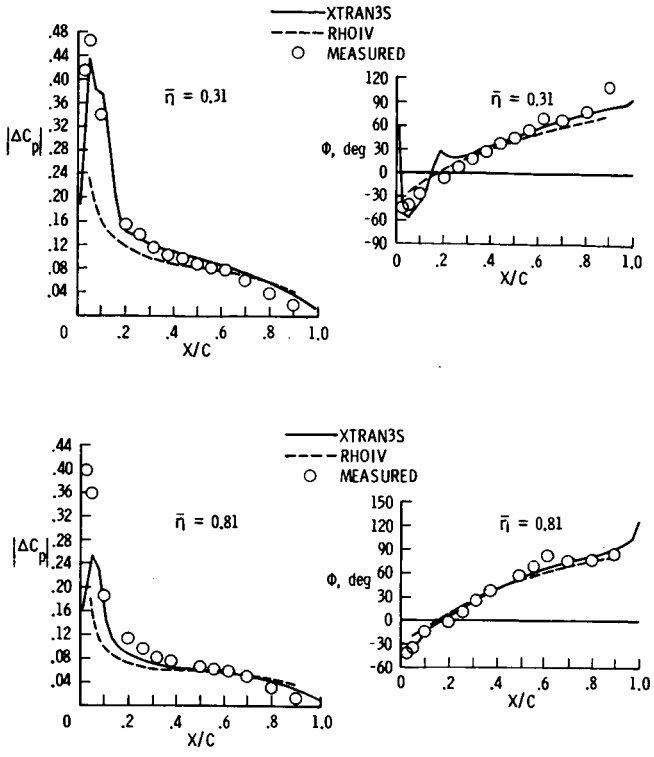

(b) Unsteady pressures

Fig. 13 Concluded.

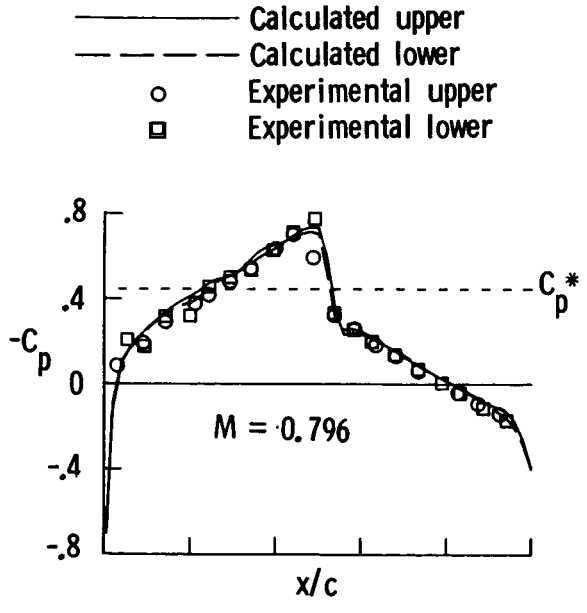

Fig. 14 Steady pressure distribution for the NACA 64A010A airfoil at M = 0.796 and α = 0 degrees.
(Edwards et al., Ref. 89)

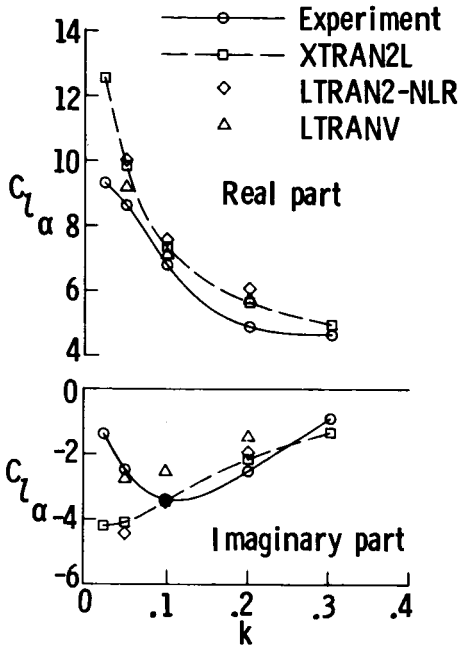

Fig. 15 Comparison of measured and calculated unsteady lift coefficient for the NACA 64A010A airfoil at M = 0.796 and α = 0 degrees.
(Edwards et al., Ref. 89)

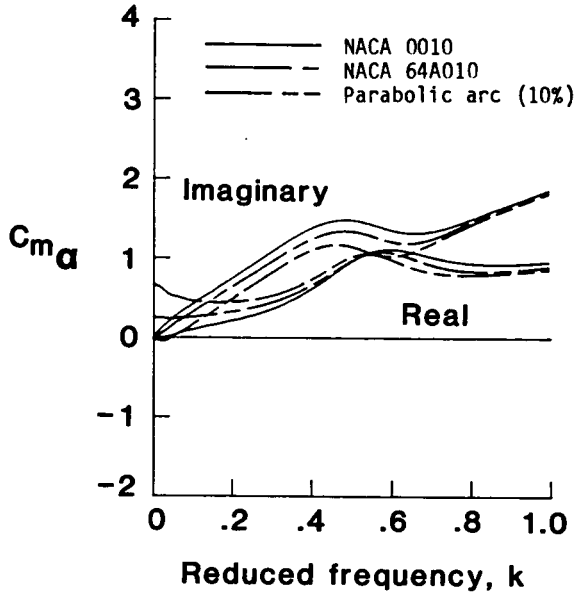

Fig. 16 Comparison of airfoil shape effects upon unsteady pitching moment coefficient for pitching oscillations at M = 0.78.
(Batina, Ref. 94)

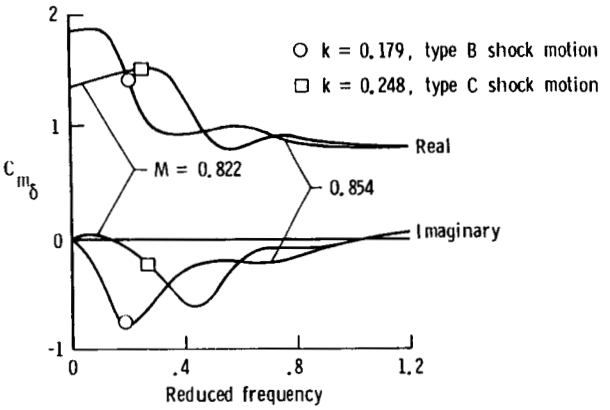

Fig. 17 Pitching moment coefficient due to flap motion for the NACA 64A006 airfoil.

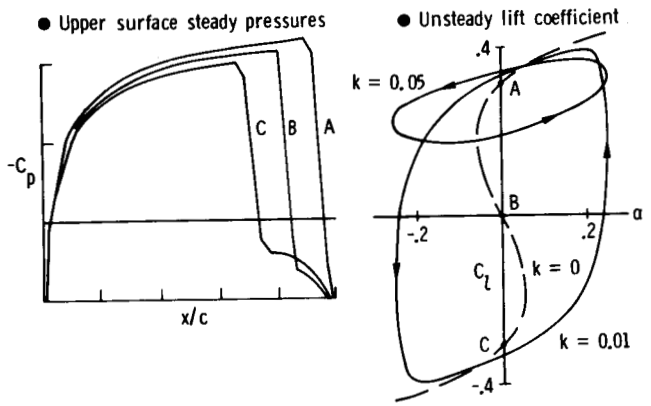

Fig. 18 Anomalous behavior of potential flow solutions for NACA 0012 airfoil at M = 0.85 and α = 0 degrees.
(Williams et al., Ref. 97)

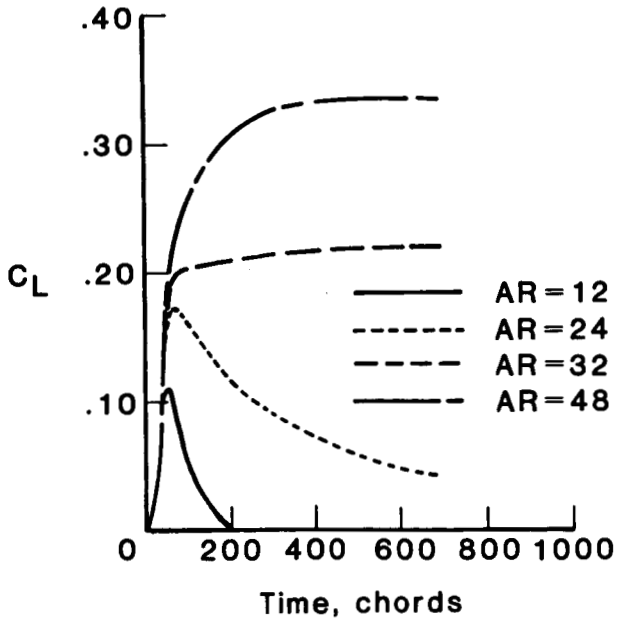

Fig. 19 Lift coefficient time histories due to pulse for NACA 0012 wing at M = 0.84 as a function of aspect ratio.
(Gibbons et al., Ref. 99)

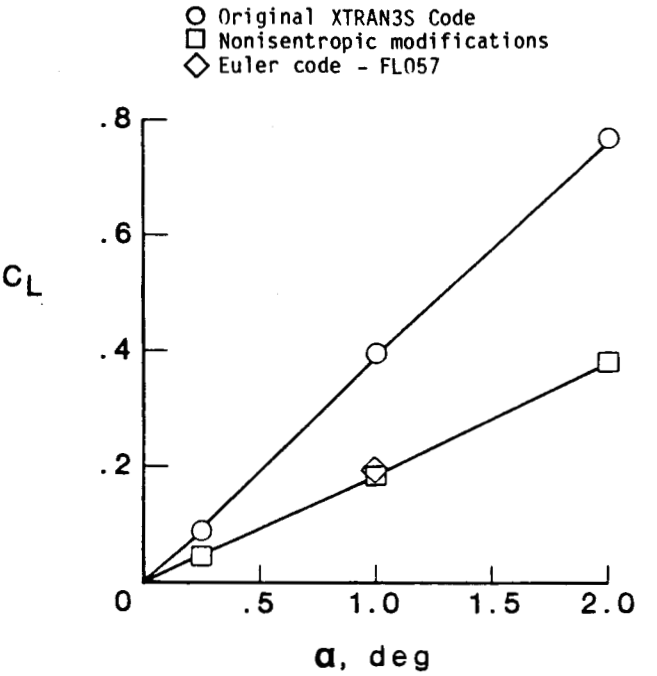

Fig. 20 Comparison of potential and Euler solutions of total lift coefficient for NACA 0012 wing with AR = 12 at M = 0.82.
(Gibbons et al., Ref. 99)

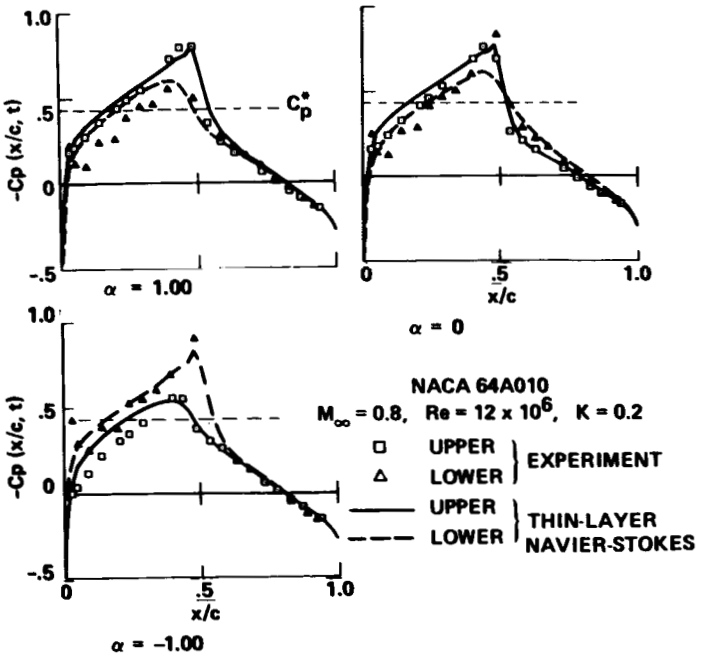

Fig. 21 Comparison of calculated and measured pressure coefficients for NACA 64A010A airfoil for moderate shock condition, α = 0° + 1° cos ωt.
(Chyu et al., Ref. 18)

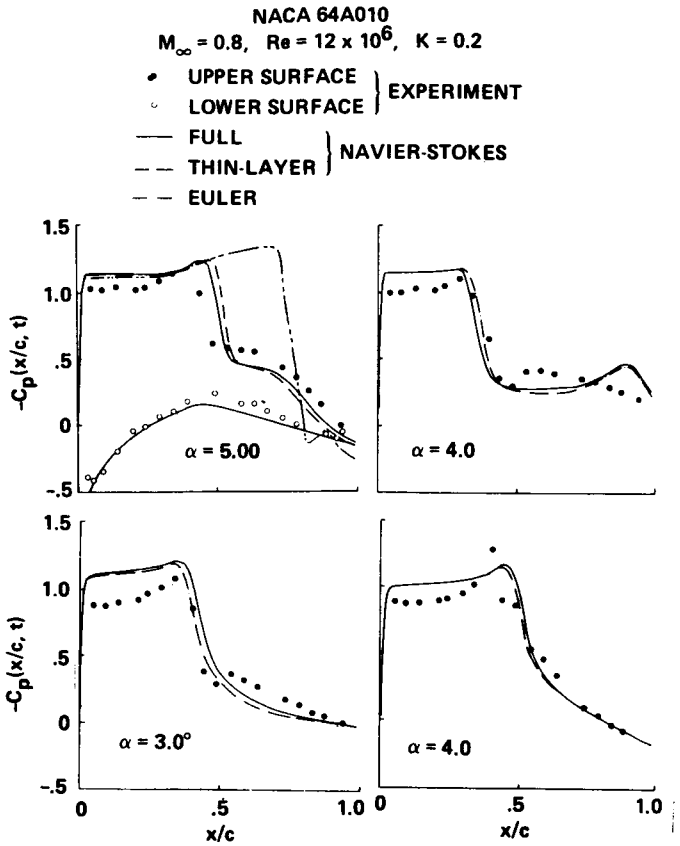

Fig. 22 Comparison of calculated and measured pressure coefficients for NACA 64A010A airfoil at shock-induced separation condition, $\alpha = 4° + 1° \cos \omega t$.
(Chyu and Davis, Ref. 19)

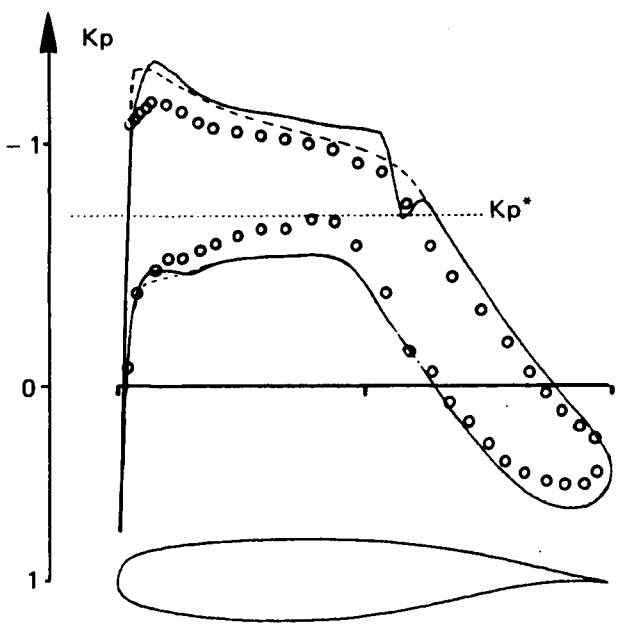

Fig. 23 Pressure coefficient distribution around the NLR 7301 airfoil in steady flow: ___ Euler calculation, and ---- hodographic method for M = 0.721, α = -0.19°. O:NLR experiment for M = 0.744, α = 0.85°.
(Sidès, Ref. 30)

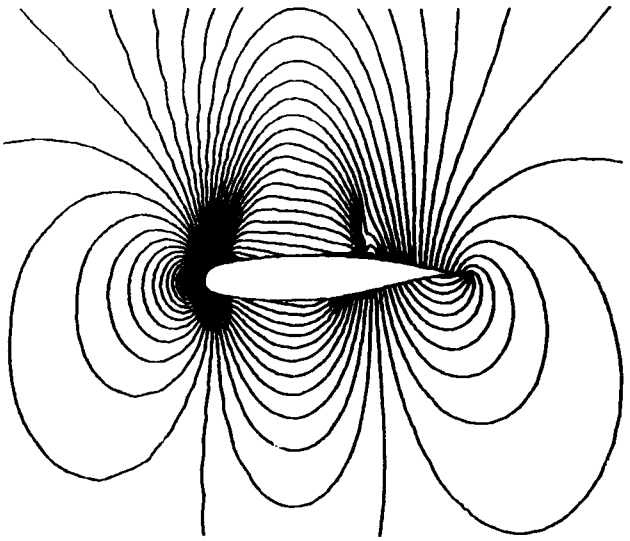

Fig. 24 Isobar lines for NLR 7301 airfoil in steady flow, under "design" conditions, M = 0.721, α = -0.19°.
(Sidès, Ref. 30)

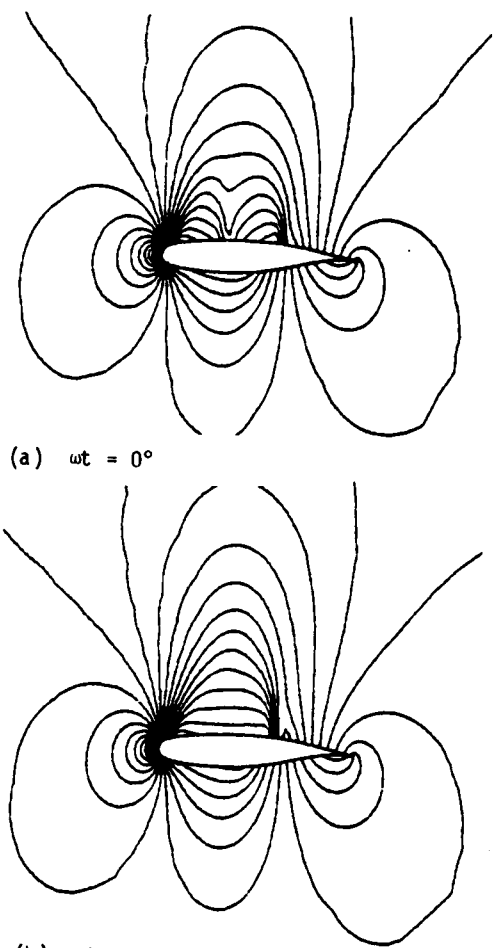

(a) $\omega t = 0°$

(b) $\omega t = 180°$.

Fig. 25 Pressure field around the NLR 7301 airfoil with oscillating flap. M = 0.721, α = -0.19°, δ = 1° sin wt , k = 0.068.
(Sidès, Ref. 30)

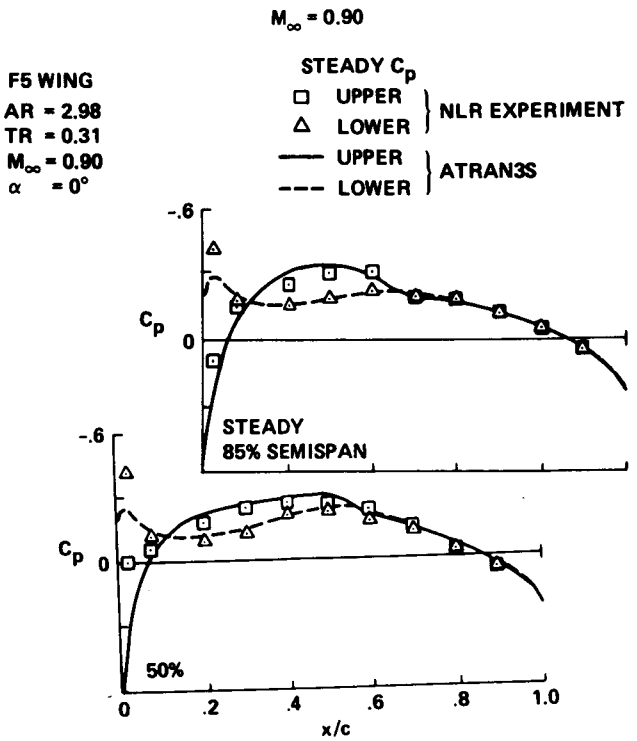

Fig. 26 Comparison of calculated and measured steady pressures for the F-5 wing model: M = 0.90.
(Guruswamy and Goorjian, Ref. 116)

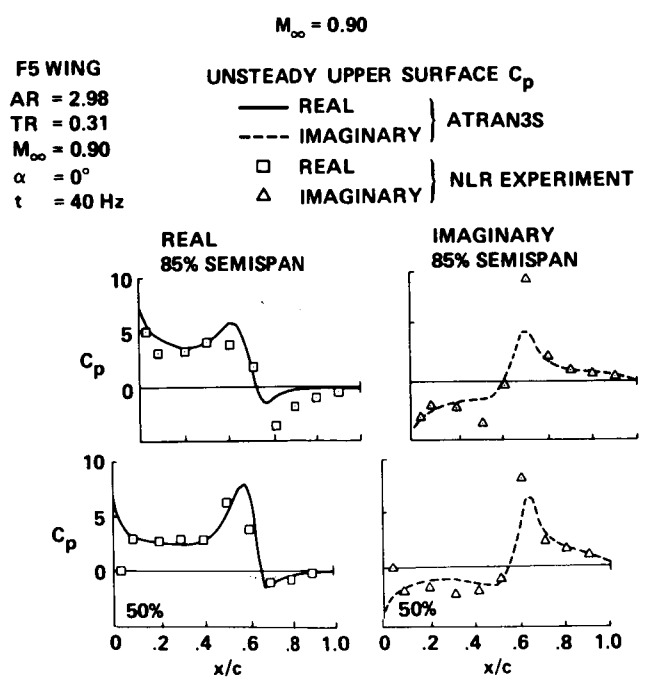

Ref. 27 Comparison of calculated and measured unsteady pressures for the F-5 wing model: M = 0.90.
(Guruswamy and Goorjian, Ref. 116)

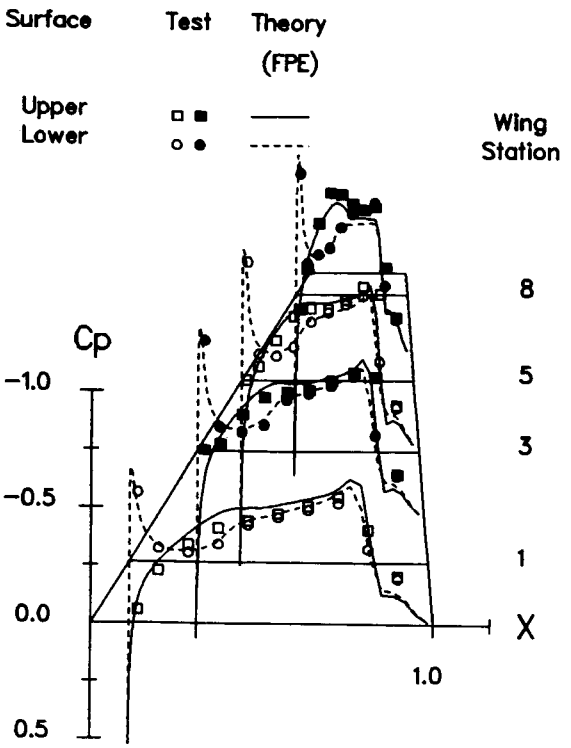

Fig. 28 Comparison of calculated and measured steady pressures for the F-5 wing model: M = 0.95.
(Malone et al., Ref. 24)

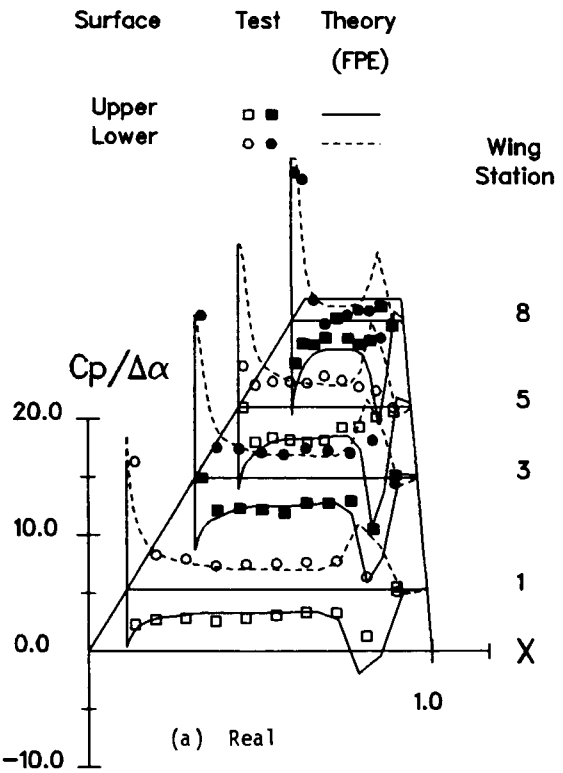

Fig. 29 Comparison of calculated and measured unsteady pressures for the F-5 wing model, M = 0.95.
(Malone et al., Ref. 24)

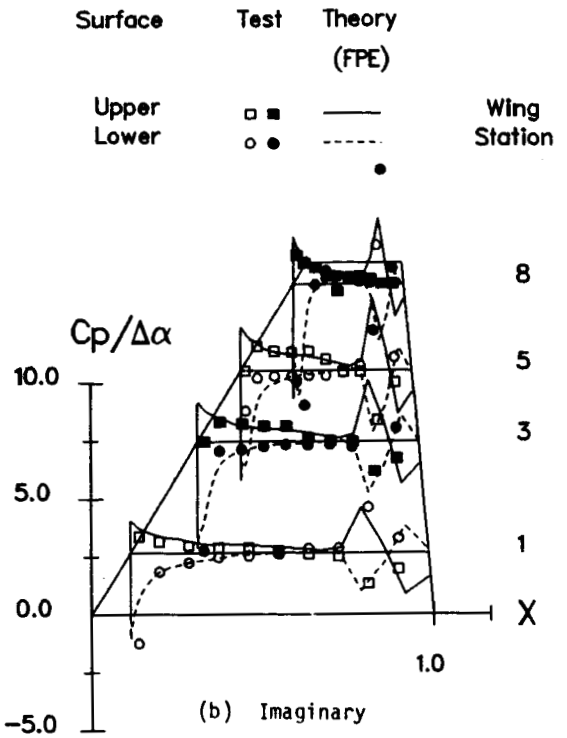

Fig. 29 Concluded.

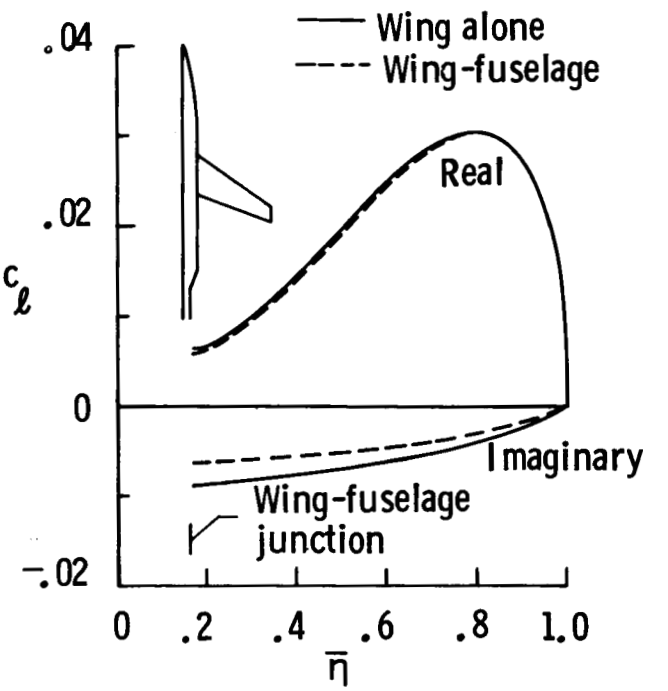

Fig. 31 Unsteady sectional lift coefficients due to assumed wing first bending mode for the RAE wing-fuselage at M = 0.91, α = 1°, and k = 0.25.
(Batina, Ref. 135)

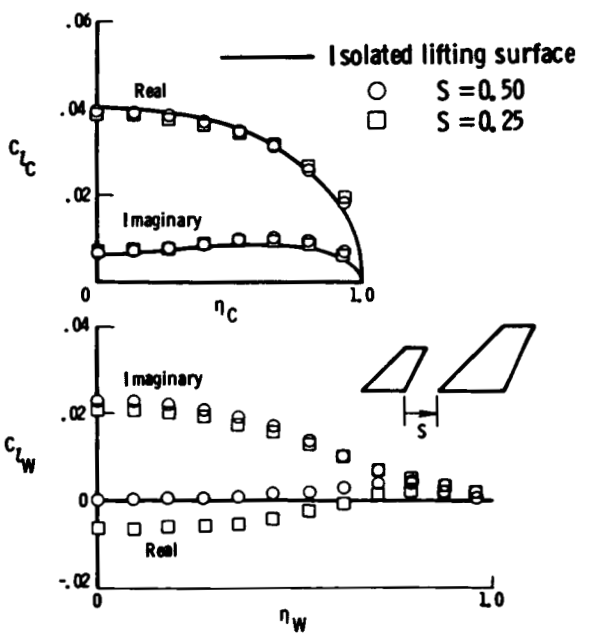

Fig. 30 Unsteady sectional lift coefficients on canard-wing configuration due to canard pitching at M = 0.90, α = 2°, and k = 0.3.
(Batina, Ref. 134)

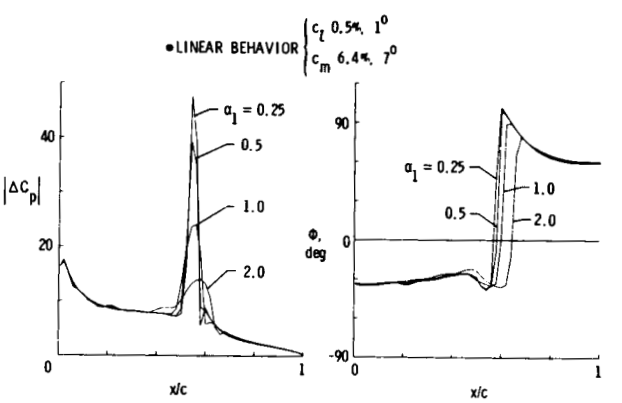

Fig. 32 Pitch amplitude effect upon normalized pressure distribution for NACA 64A010A airfoil at M = 0.78, α = 0°, and k = 0.15.
(Bland and Edwards, Ref. 83)

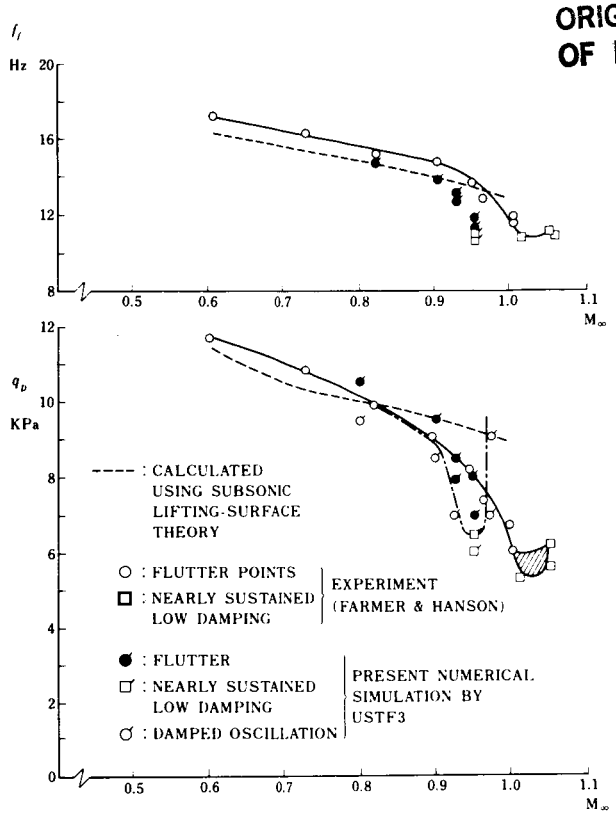

Fig. 33 Comparison of calculated and experimental flutter boundaries for a TF-8A supercritical wing flutter model. (Isogai and Suetsugu, Ref. 71)

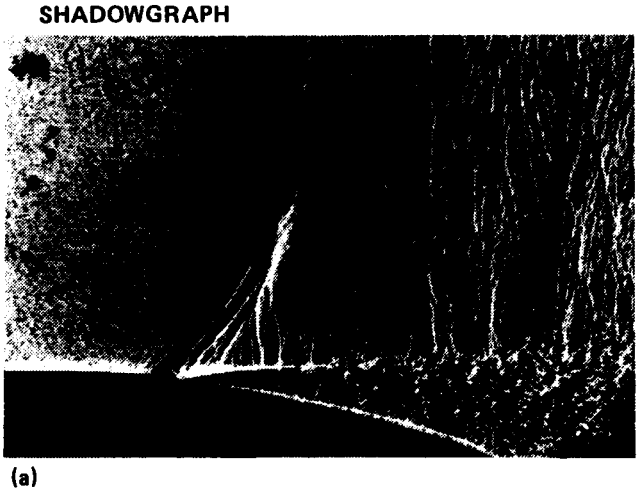

Fig. 34 Comparison of Navier-Stokes computations of Coakley with experiments of McDevitt for steady shock-induced boundary separation, M = 0.785, Re = 11 x 10^6. (Coakley, Ref. 145)

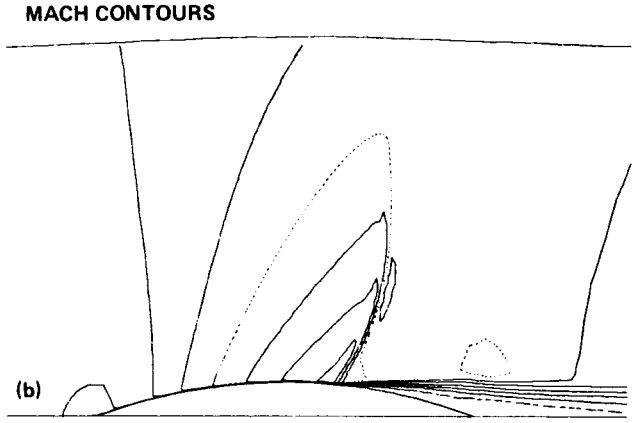

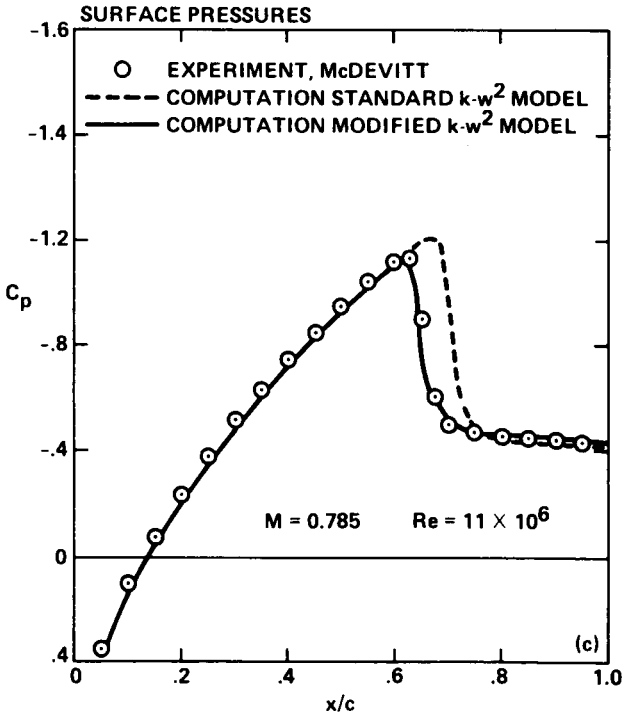

Fig. 34 Concluded.

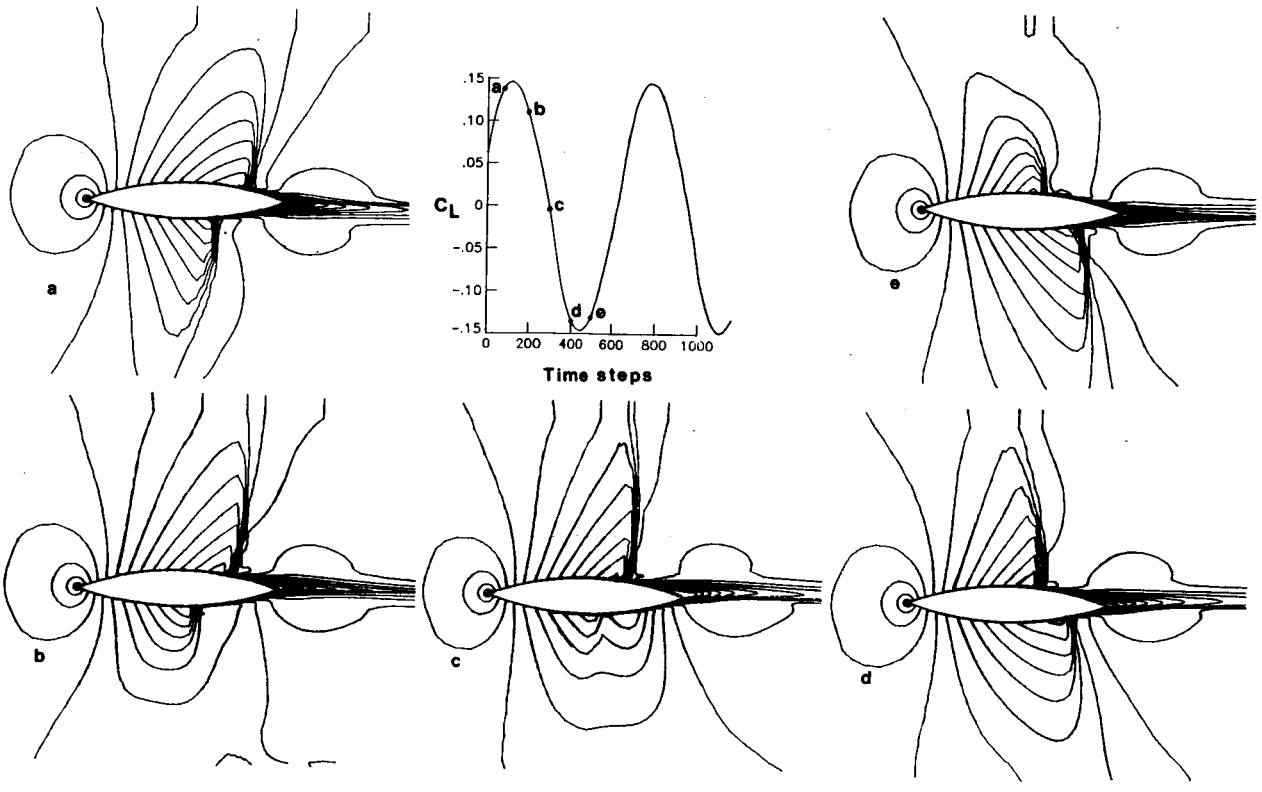

Fig. 35 Calculated periodic oscillation for 18% biconvex airfoil with implicit thin-layer Navier-Stokes code, M = 0.78, Re = 11 x 10^6, k = 0.406.

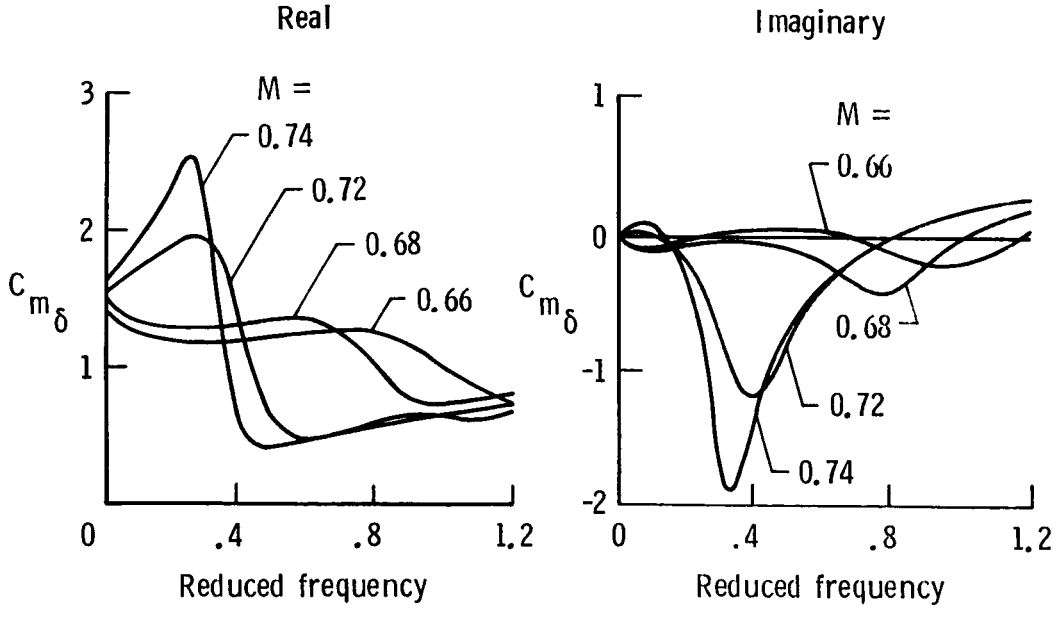

Fig. 36 Calculated pitching moment coefficient for 18% biconvex airfoil with non-isentropic TSD code.

Standard Bibliographic Page

1. Report No.	2. Government Accession No.	3. Recipient's Catalog No.
NASA TM-89106		

4. Title and Subtitle	5. Report Date
Computational Methods for Unsteady Transonic Flows	March 1987
	6. Performing Organization Code: 505-63-21-01
7. Author(s): John W. Edwards and J. L. Thomas	8. Performing Organization Report No.
9. Performing Organization Name and Address: NASA Langley Research Center, Hampton, Virginia 23665-5225	10. Work Unit No.
	11. Contract or Grant No.
12. Sponsoring Agency Name and Address: National Aeronautics and Space Administration, Washington, DC 20546	13. Type of Report and Period Covered: Technical Memorandum
	14. Sponsoring Agency Code

15. Supplementary Notes

Presented at the AIAA 25th Aerospace Sciences Meeting, January 12-15, 1987, Reno, Nevada. AIAA Paper No. 87-0107.

16. Abstract

Computational methods for unsteady transonic flows are surveyed with emphasis upon prediction. Computational difficulty is discussed with respect to type of unsteady flow; attached, mixed (attached/separated) and separated. Significant early computations of shock motions, aileron buzz and periodic oscillations are discussed. The maturation of computational methods towards the capability of treating complete vehicles with reasonable computational resources is noted and a survey of recent comparisons with experimental results is compiled. The importance of mixed attached and separated flow modeling for aeroelastic analysis is discussed and recent calculations of periodic aerodynamic oscillations for an 18 percent thick circular arc airfoil are given.

17. Key Words (Suggested by Authors(s))	18. Distribution Statement
Transonic Unsteady Aerodynamics Aeroelasticity Flow Oscillations	Unclassified - Unlimited Subject Category - 02

19. Security Classif.(of this report)	20. Security Classif.(of this page)	21. No. of Pages	22. Price
Unclassified	Unclassified	30	A03

For sale by the National Technical Information Service, Springfield, Virginia 22161